Radio/mm/sub-mm observations of AGB stars

Hans Olofsson
Space, Earth and Environment, Chalmers, Sweden
Onsala Space Observatory

AGB stars

- Post central-helium burning stars ascending the second red giant branch (the asymptotic giant branch).
- Mass range ≈ 0.8 - 8 $M_\odot$.
- Three chemical types: M- (C/O≈0.5 by number), S- (C/O≈0.5-1), C-stars (C/O>1).
- C-stars are found in the range 1.5 < M < 4 $M_\odot$.
- Pulsating: Irregular, Semi-regular, and Long-period (Mira) variables.
- Intense stellar winds (10^{-8} to $>10^{-4}$ $M_\odot$/yr), and important contributors of elements and dust grains to the ISM.
- The progenitors of Planetary Nebulae.

Central to this talk

Stellar surfaces & extended atmospheres

How do they look like?

We have reached the time when radio interferometers can resolve structures on the surface of a red giant star.

This will put important constraints on the modelling of the stars themselves and the initial conditions for mass loss.

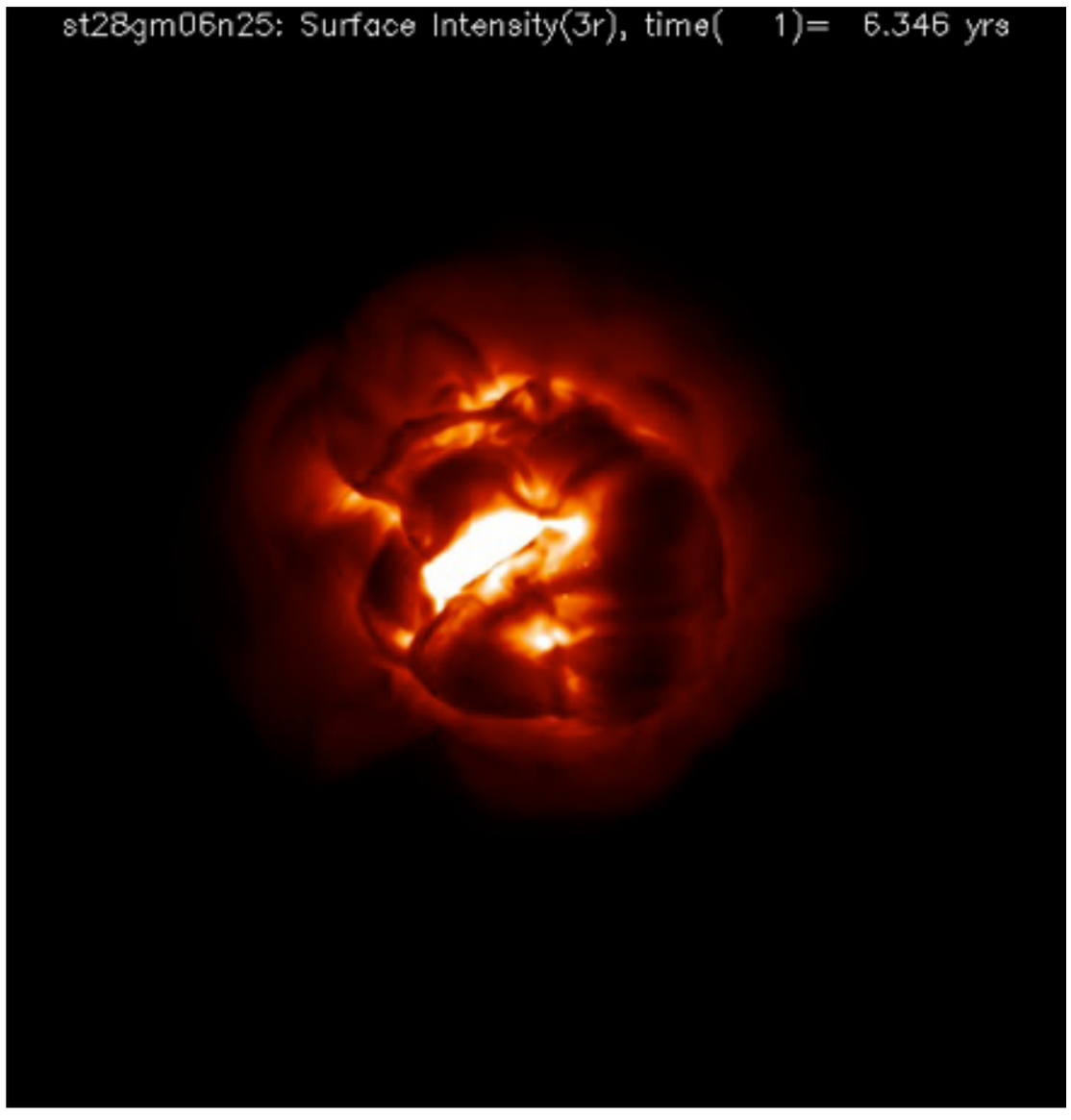

Do they look like this?

3D simulations have come a long way, and they include convection, pulsation, and dust condensation

Freytag et al., A&A 600, A137 (2017)

Pioneering work revealed a radio photosphere

- Reid & Menten, ApJ 476, 327, 1997;
  W Hya (M-star) ≈80 mas at 22 GHz
- Reid & Menten, ApJ 671, 2068, 2007;
  o Ceti, R Leo, and W Hya (M-stars) ≈55 mas at 43 GHz
- O'Gorman et al., A&A 580, A101, 2015
  α Ori (RSG)

The size depends on the frequency!

This is what is expected. The surface where $\tau_{ff} \approx 1$ is wavelength dependent ($\nu^{-2.1}$).

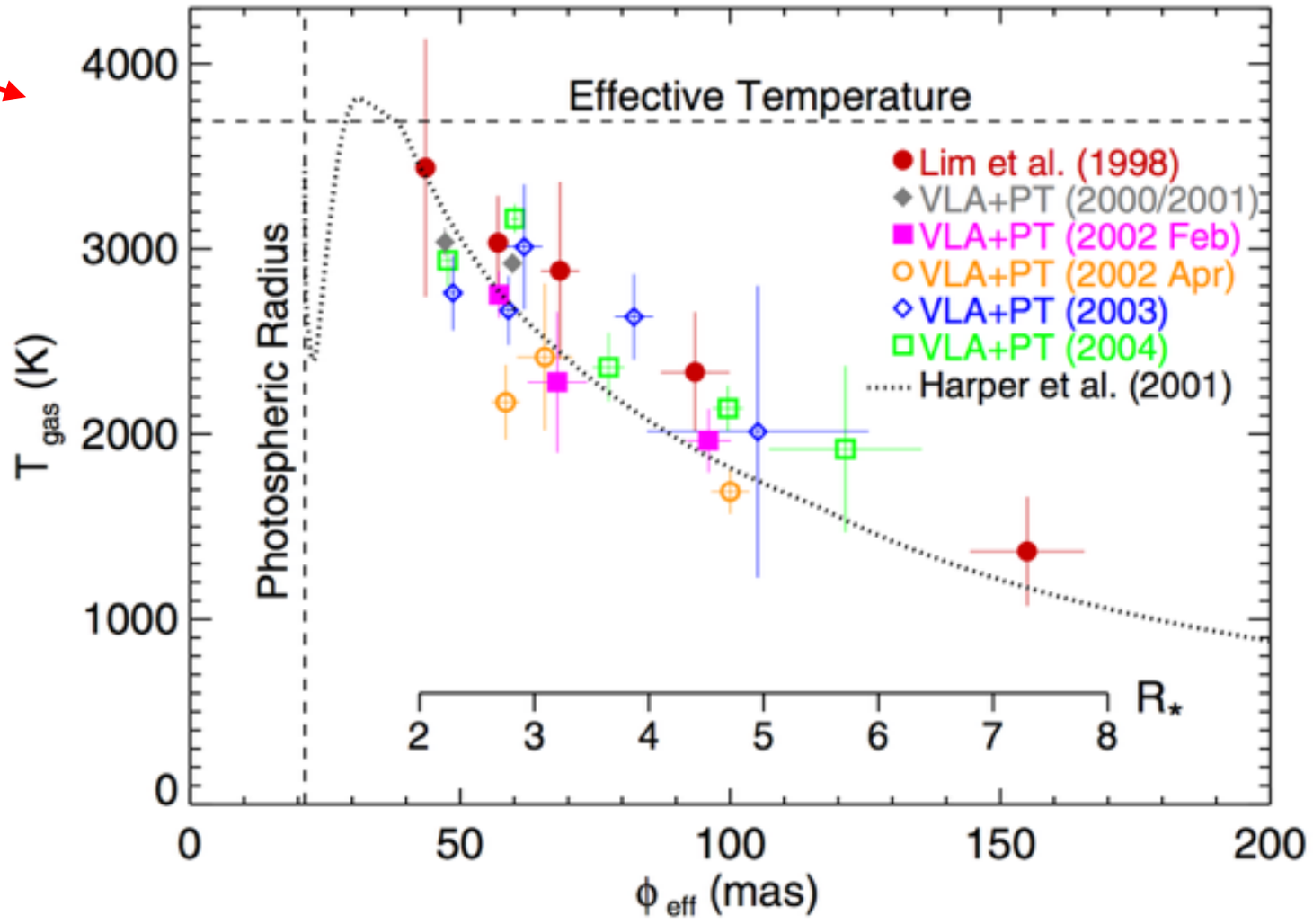

A radio photosphere

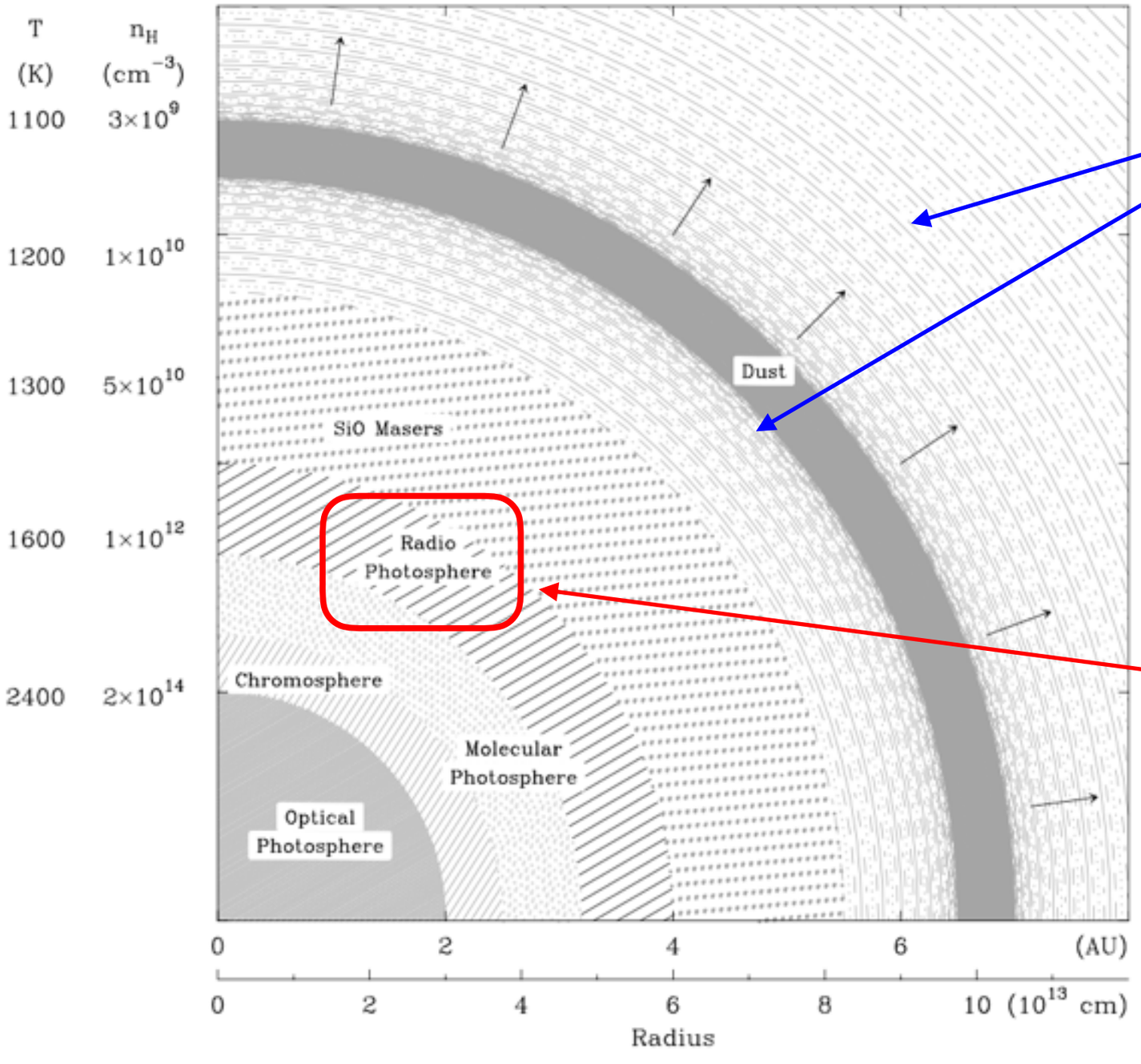

The regions where the mass-loss characteristics ($\dot{M}$ and v_∞) are determined.

The location depends on v.

A very good probe of the extended atmosphere!

Reid & Menten, ApJ 476, 327 (1997)

ALMA higher-frequency observations of W Hya

CO(v=1, J=3-2)
E_{up} ≈ 3120 K

photospheric disk

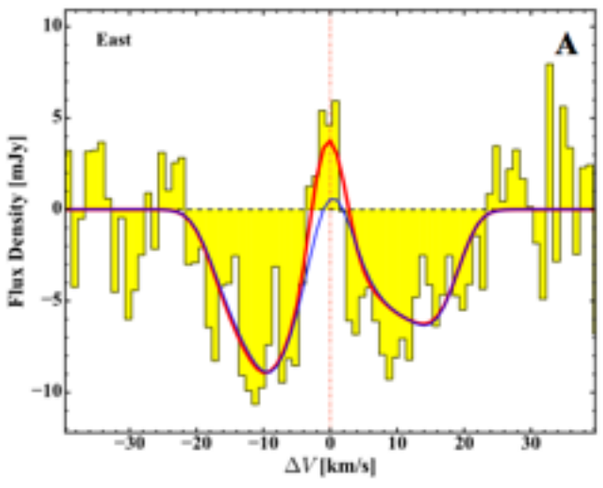

Eastern side

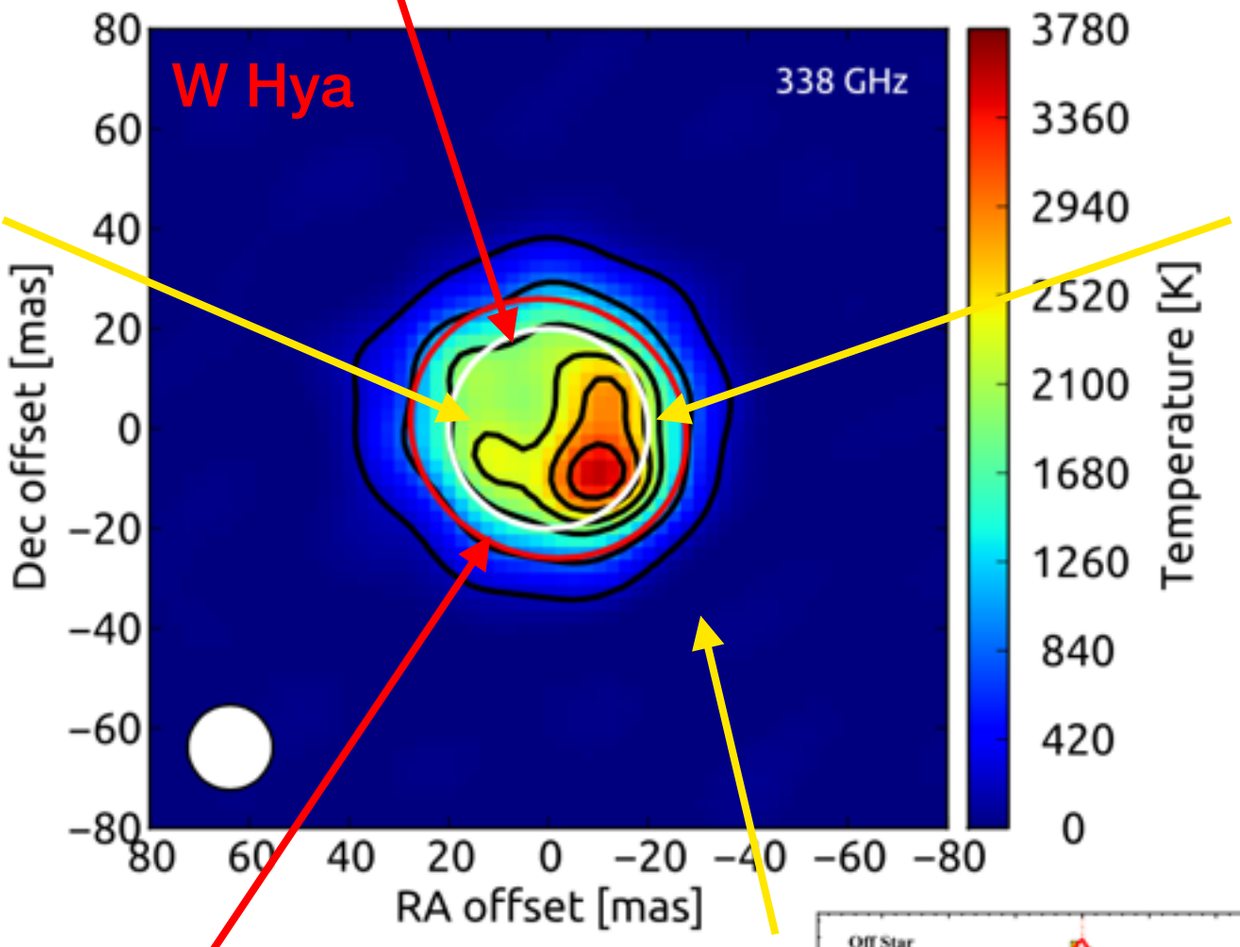

338 GHz disk
(≈ photospheric temperature)

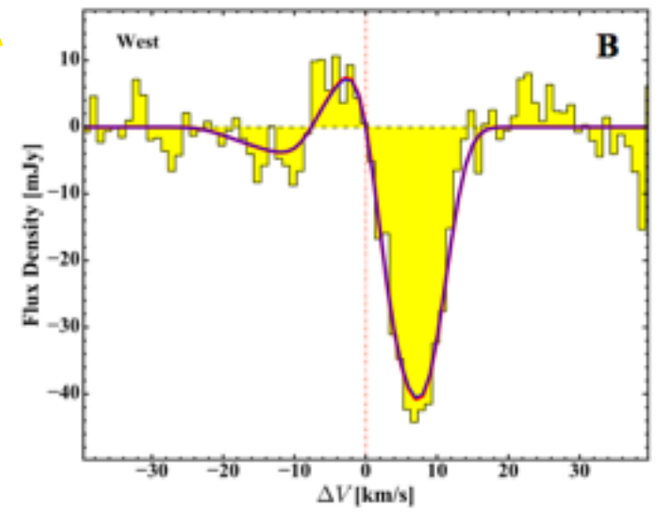

Western side

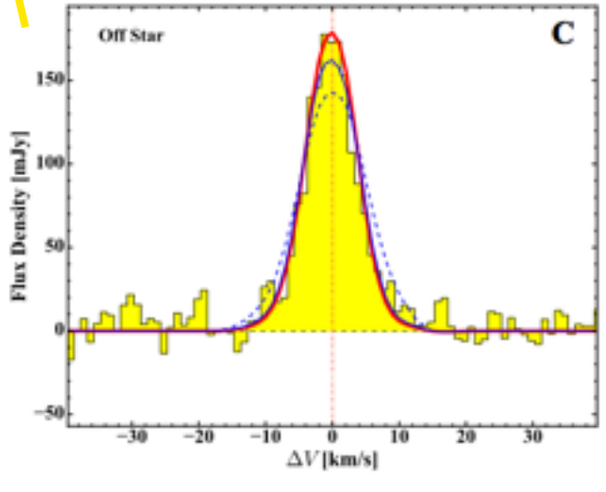

Outside disk

Vlemmings et al. , Nature Astronomy, in press

Conclusions from this

- Gas with $T_b > 5x10^4$ K (chromospheric characteristics) having a low volume filling factor.
- Shock velocities of ≈ 20 km/s.
- A warm (= 2900 K, photosphere is 2500 K) “stationary” molecular gas layer. Mass is enough for the mass-loss rate over ≈1000 yr (=> all gas experience shock heating).
- A cool (≈ 900 K) molecular gas layer in the region of dust condenstation.

Presently, not all of this is consistent with models!

This type of observations are difficult because:

- the stars are variable and multi-epoch data are required
- in addition, these are required at multi-wavelengths

Mass loss

The importance of AGB mass loss

The mass-loss rate determines the AGB evolution, in particular the number of dredge-ups and the maximum light reached.

It is therefore crucial to determine its properties for stars in different phases of its AGB evolution.

However, the study is complicated by the fact that the mass-loss rate depends on stellar parameters like M, L, T_{eff}, and Z and their evolution with time on the AGB.

Any sample of (detected) stars will therefore be inhomogeneous and general conclusions are not always easily drawn.

The best mass-loss-rate estimator for these stars is CO rotational line emission from their circumstellar envelopes (CSEs).

Mass-loss rate & expansion velocity

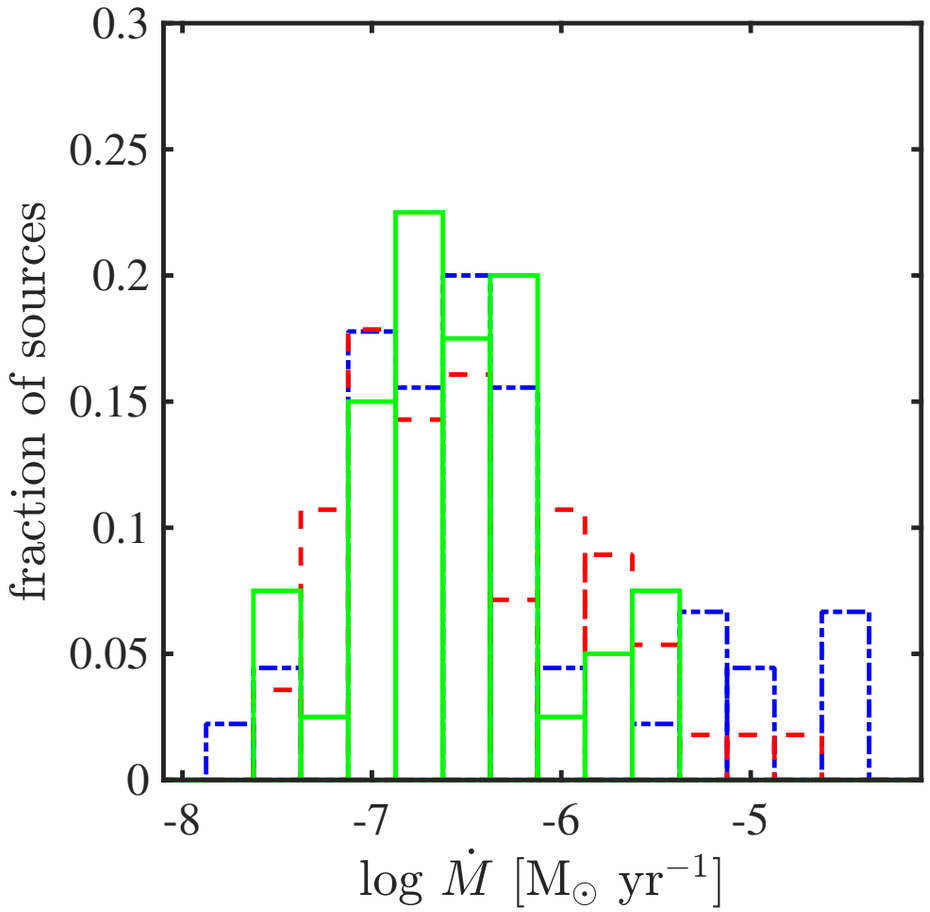

CO data towards nearby stars:
73 M-stars
40 S-stars
61 C-stars

+

Radiative transfer CO line modelling

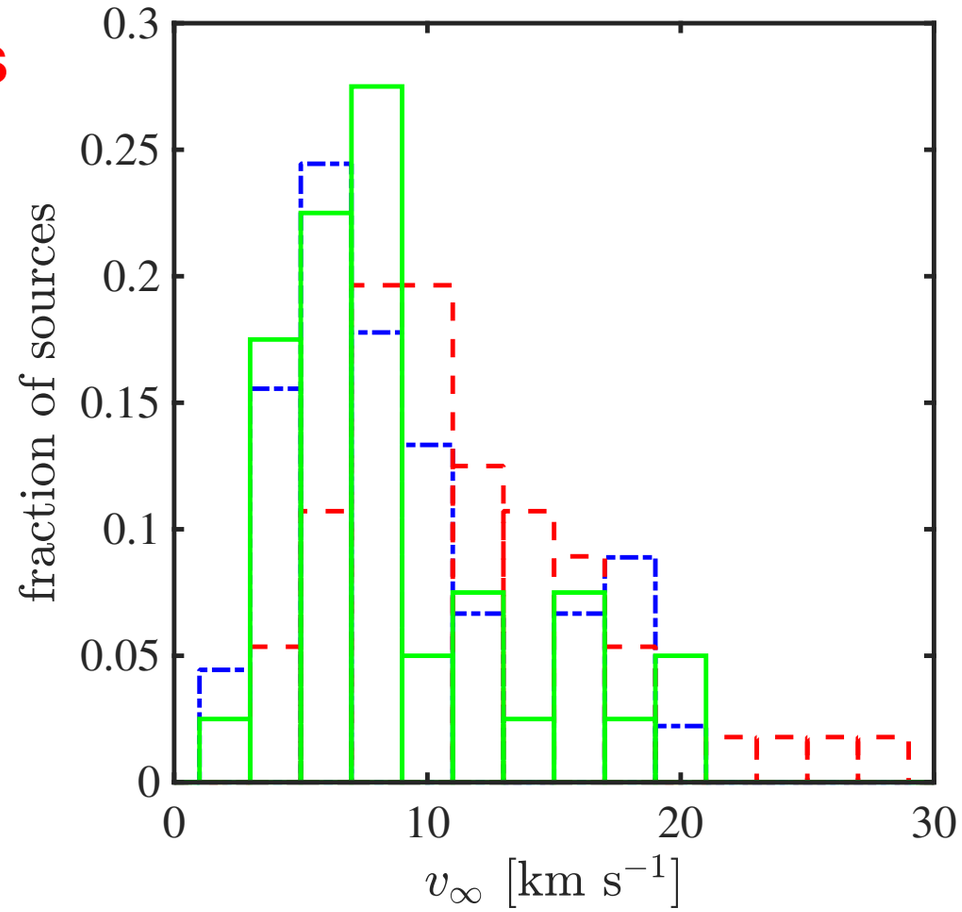

- Mass-loss rate independent of chemistry
- Expansion velocity (on average) somewhat higher for C-stars
- The mass return is dominated by the rare (<5%) high-mass-loss-rate objects (> 10^{-5} $M_\odot$/yr)

Interferometric data can improve the accuracy of mass-loss-rate estimates.

Ramstedt et al., A&A 499, 515 (2009)

Temporal evolution: Is there a superwind?

Various evidences point to a mass-loss rate that increases substantially at the end of the AGB evolution.

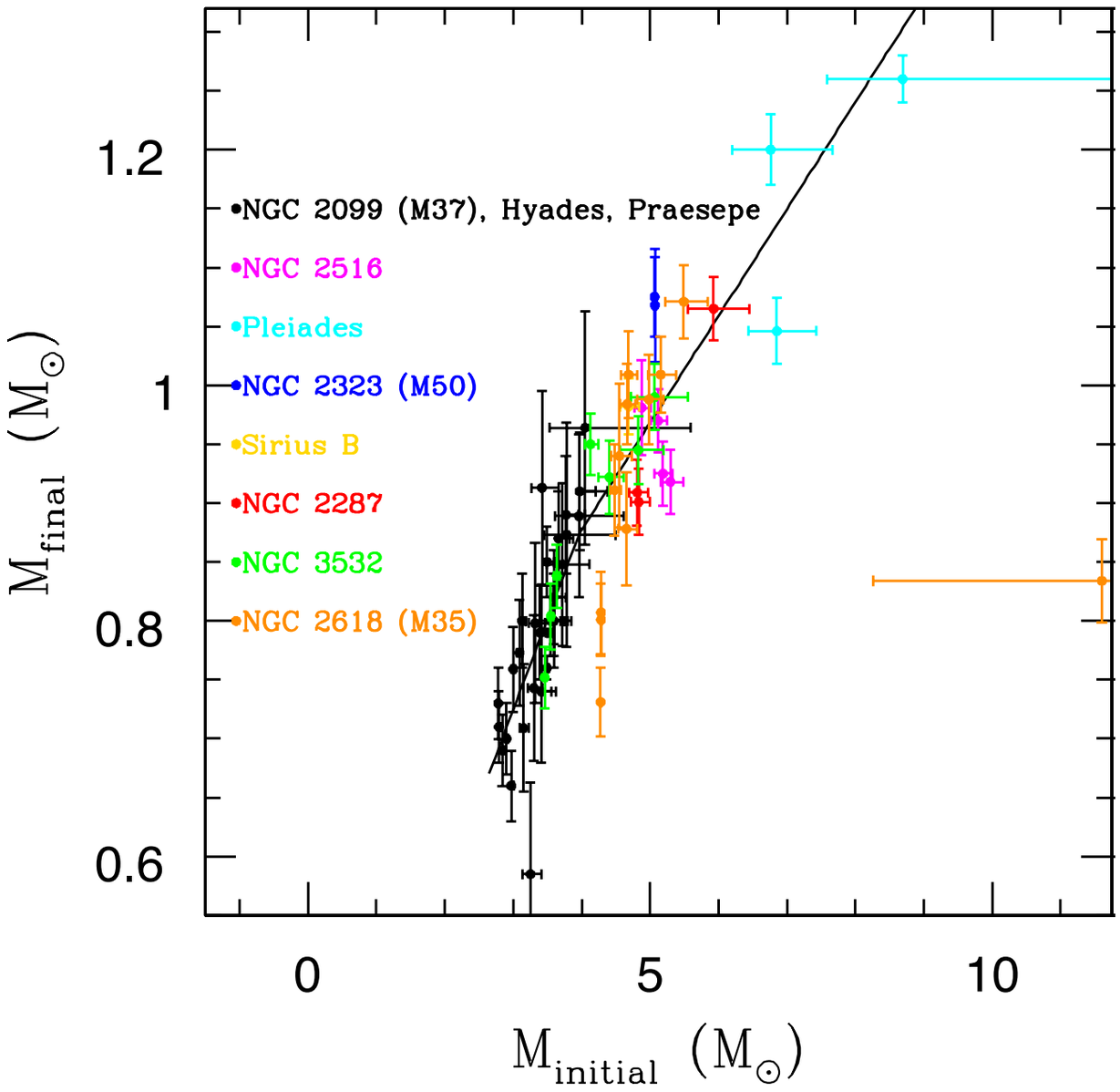

Initial-final mass relation

They must lose M_i - M_f.

This can be more than 80% of M_i.

Justtanont et al. (A&A 556, A101, 2013):

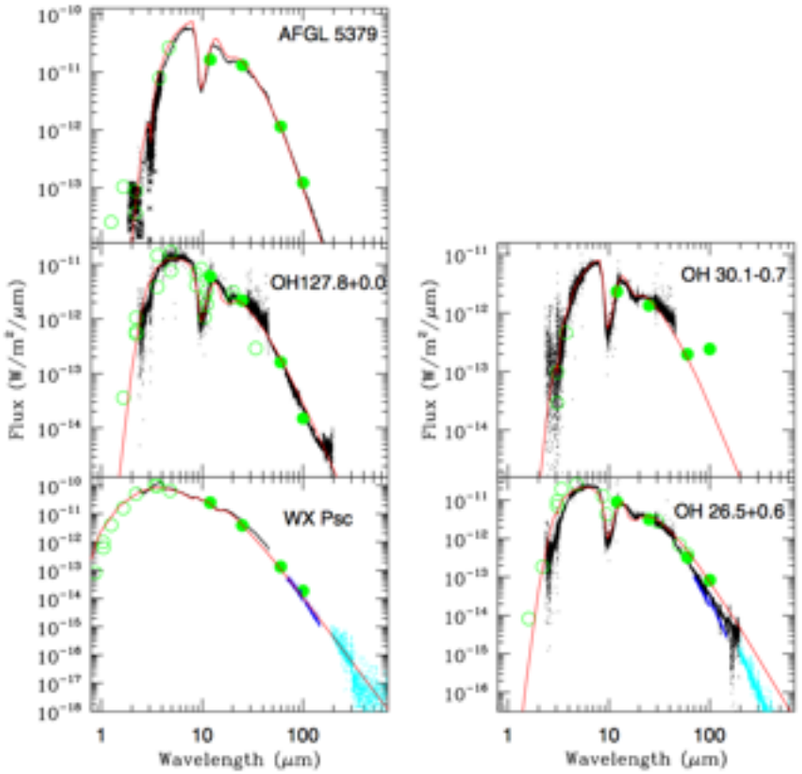

Fig. 1. SED fits for the sample stars (solid line) to the ISO spectra (black dots) and photometric points from IRAS (filled green circles). The PACS (blue dots) and SPIRE (cyan dots) spectra are also plotted when available. The published photometric data (open circles) are taken from Dyck et al. (1974) and Epchtein et al. (1980) for WX Psc, Persi et al. (1990) for OH 127.8+0.0, Garcia-Lario et al. (1997) and Lepine et al. (1995) for AFGL 5379, Werner et al. (1980) for OH 26.5+0.6, and Justtanont et al. (2006) for both OH 26.5+0.6 and OH 30.1-0.7.

4 extreme OH/IR-stars (M ≈ 5 $M_\odot$):

$$\dot{M}_{\rm dyn} \approx (2-10) \times 10^{-4}\ {\rm M_\odot\ yr^{-1}}$$

but $\dot{M} \approx 3 \times 10^{-6}\ {\rm M_\odot\ yr^{-1}}$ beyond (1-3)x10^{16} cm to explain the low-J CO lines.

With v_∞ ≈15 km/s this means that the SW phase has lasted for only ≈ 200 – 600 yr.

Amount of mass lost during the SW is of the order 0.1 $M_\odot$, but they need to lose about 4 $M_\odot$ in total.

Independent evidence:

de Vries et al. (A&A 561, A75, 2014)
used the 69 μm feature to estimate that the outer radius of the SW must be < 3x10^{16}cm (≈ 500 yr).

Are there several SW phases for an individual star?

Measure the duration using ALMA and CO lines!

$$\dot{M}(M, L, T_{\rm eff}, P, Z)$$

A mass-loss-rate prescription where the mass-loss rate can be calculated from stellar characteristics are important for stellar population and chemical yields modelling.

In particular, for estimating the contribution from AGB stars to galactic light, dust production, and element synthesis.

Observationally a very difficult problem due to observational biases and the correlation of different stellar parameters, meaning very difficult to determine dependences on for instance M, L, and $T_{\rm eff}$.

A mass-loss-rate prescription

Best correlation is that between mass-loss rate and pulsational period.

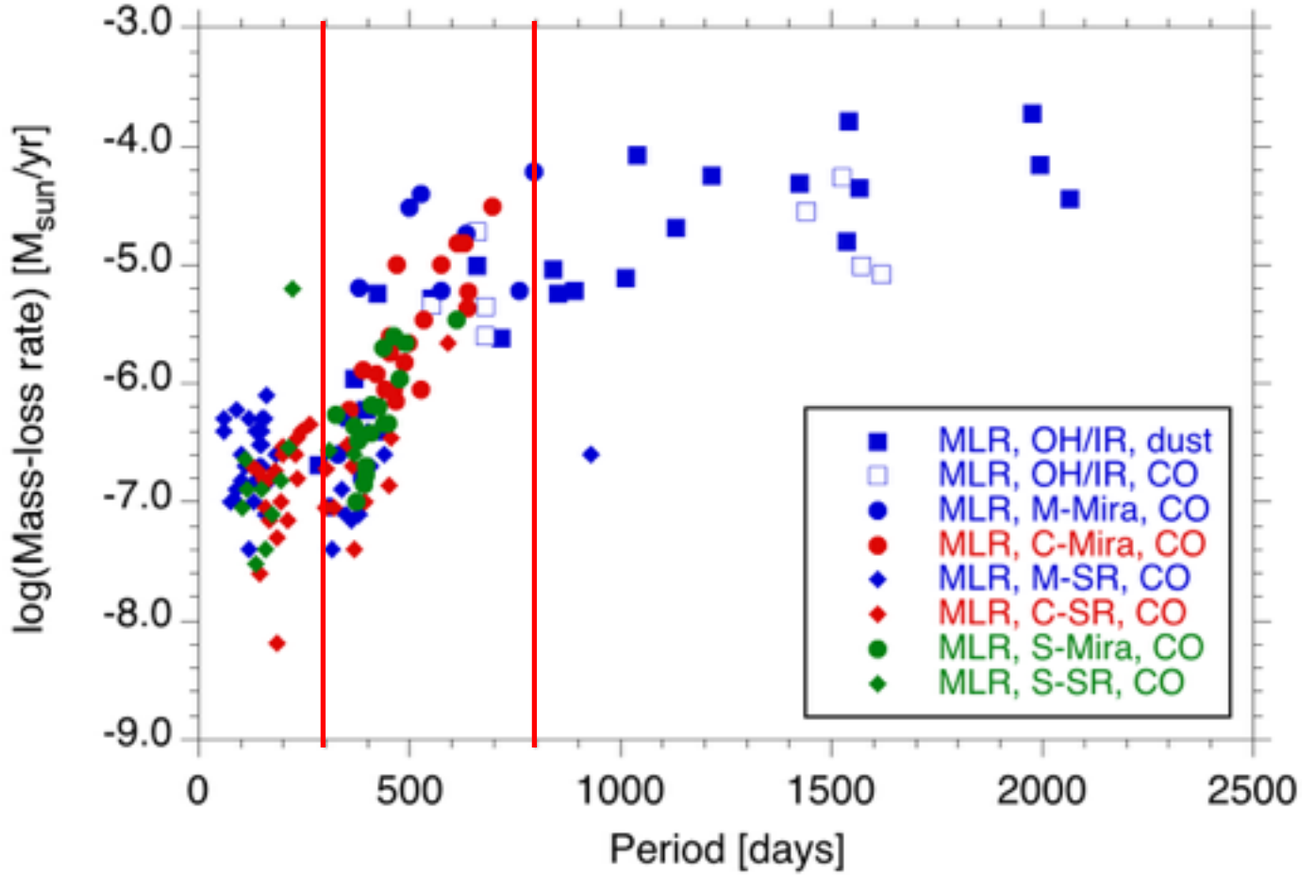

The correlation in the range $300^d < P < 800^d$ is most likely a combined effect of decreasing mass and increasing luminosity.

This lead to the best mass-loss-rate prescription so far:

$$\log \dot{M}(M_\odot \text{ yr}^{-1}) = -11.4 + 0.0123P \text{ (days)} .$$

$$\log P \text{ (days)} = -2.07 + 1.94 \log R/R_\odot - 0.9 \log M/M_\odot$$

Vassiliadis & Wood
ApJ 413, 641 (1993)

An object, caught in action when the changes in stellar parameters are known, may be the “Rosetta stone” in this context.

Mass-loss rate variation during and after a thermal pulse, the He-shell flash phenomenon.

^{12}CO(3-2) image of R Scl (ALMA)
Maercker et al. Nature 409, 232 (2012)

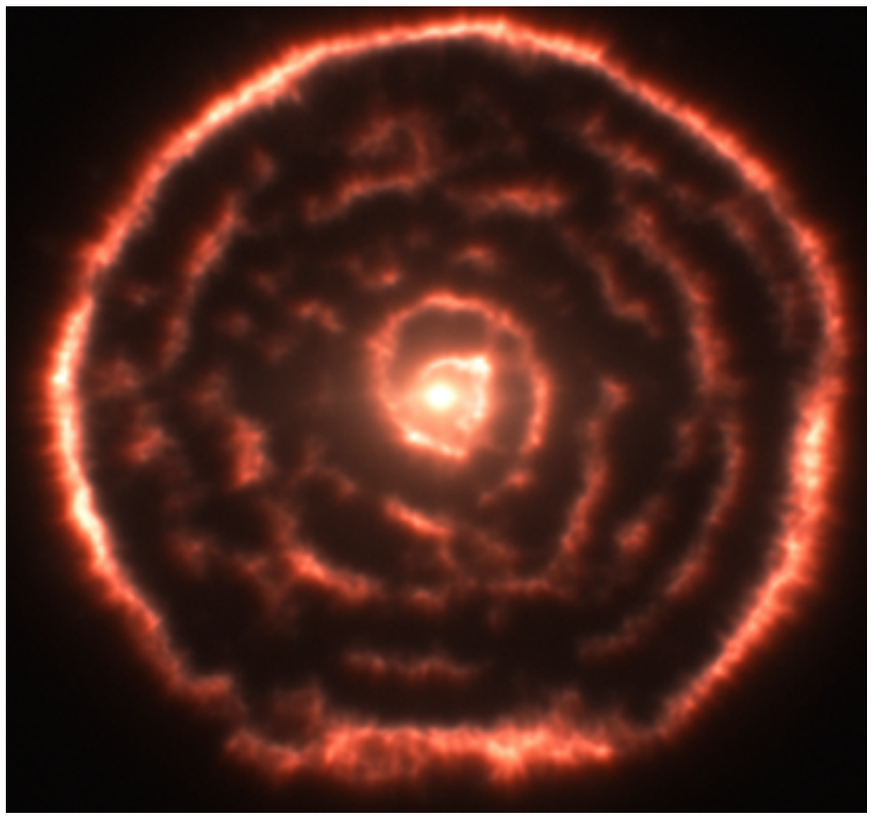

^{12}CO(2-1) image of U Ant (ALMA),
Kerschbaum et al. A&A 605, A116 (2017)

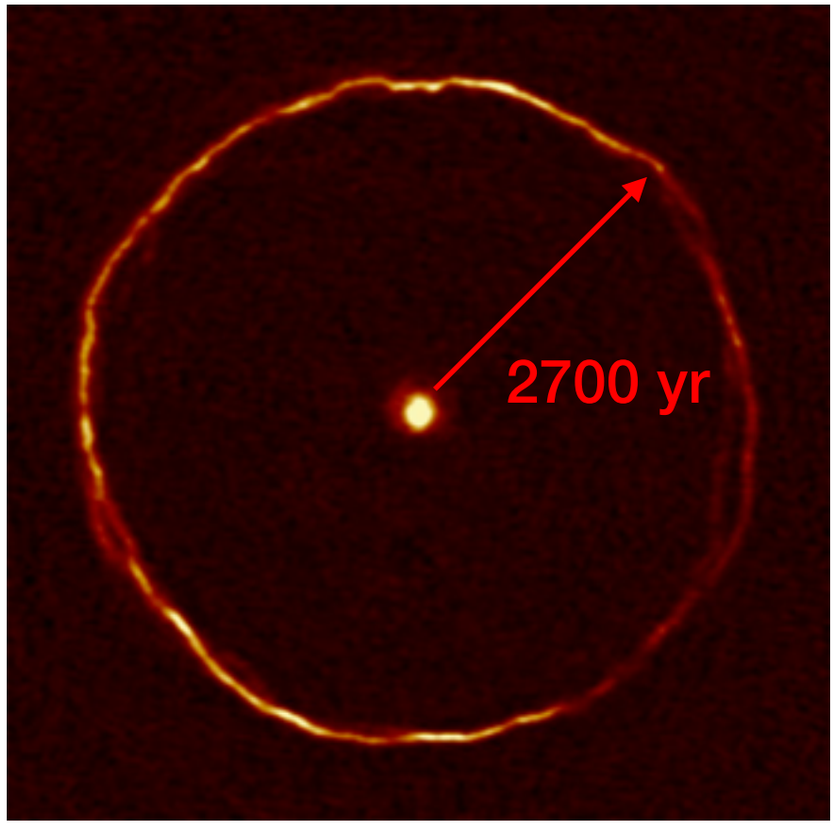

The mass-loss-rate history may be the same for these two objects. It is the effect of the companion to R Scl that makes the CO line emission from the intershell region detectable in that case.

Central to astrophysics is the mass-loss-rate dependence on metallicity.

This requires samples of more distant (extragalactic) sources observed in CO, hence ALMA !!

Lower Z means:

- Lower CO abundance in both M- and C-stars.
- Often smaller CO envelopes due to more intense UV field and lower CO abundance.
- Both effects lower the CO line intensities.

Four C-stars detected in CO in the LMC using ALMA.

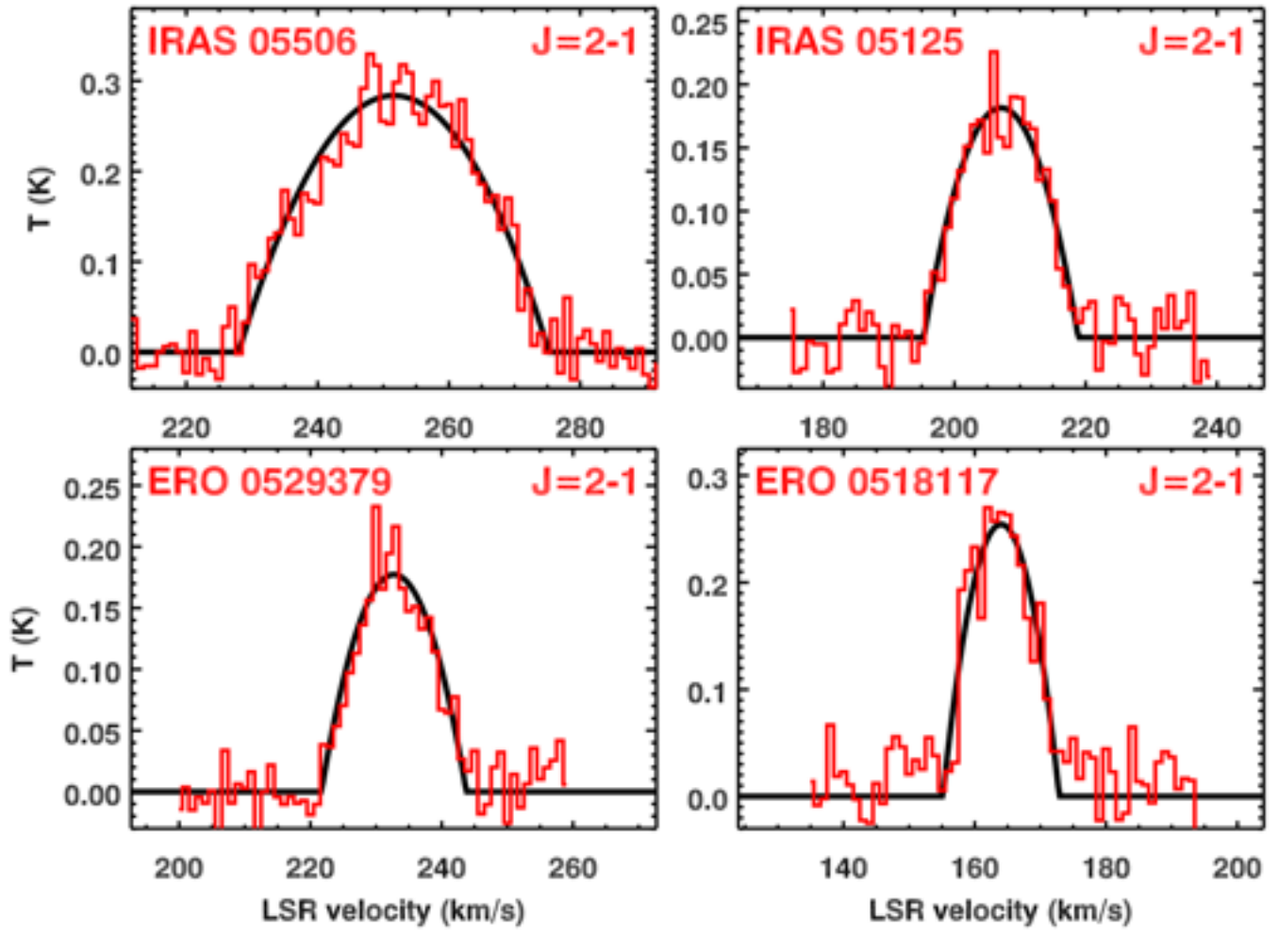

The LMC has 0.5 $Z_\odot$, and it would be very interesting to try also the SMC at 0.2 $Z_\odot$.

It will most likely be difficult to go beyond the MCs to detect AGB stars in CO rotational line emission, even with ALMA.

Groenewegen et al., A&A 596, A50 (2016)

Mass-loss rate vs. expansion velocity

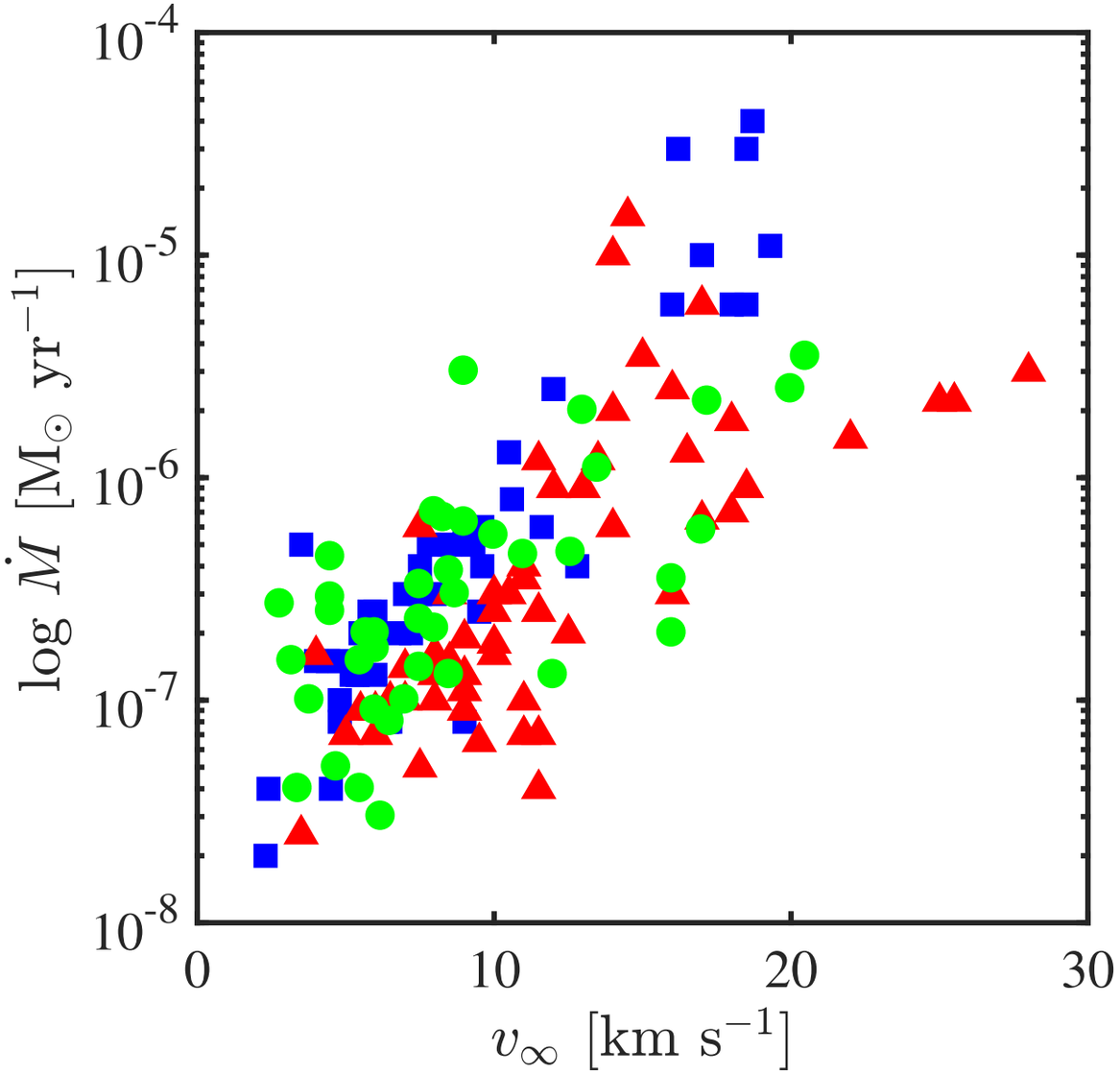

CO data towards
73 M-stars
40 S-stars
61 C-stars

Important constraint on any viable mass-loss mechanism !!

Ramstedt et al., A&A 499, 515 (2009)

The velocity profile

Decin et al. (A&A 521, L14, 2010) used Herschel CO, H_2O, SiO, to derive velocity profile for IK Tau.

v(r)

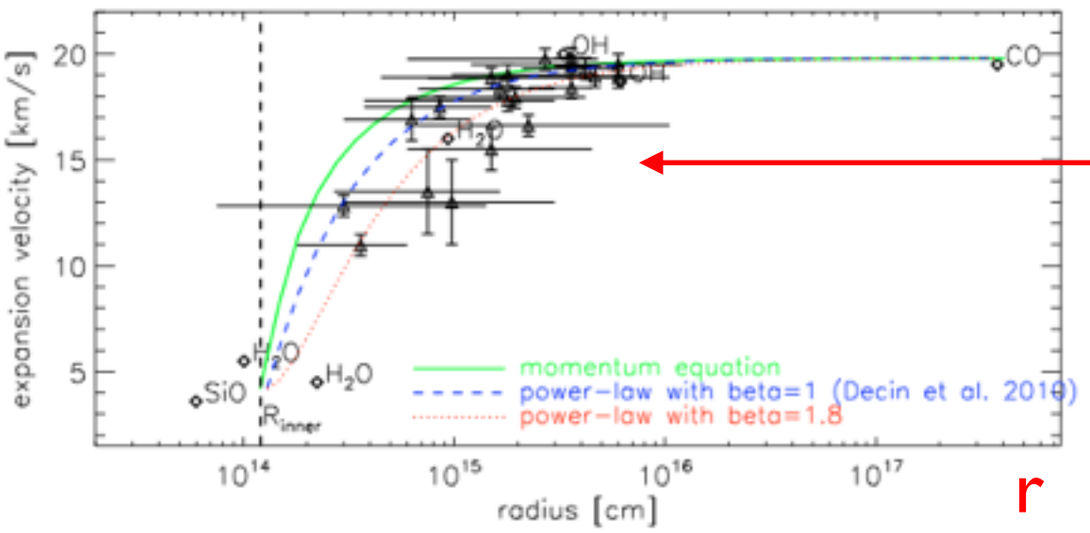

r

$$v(r) \simeq v_0 + (v_\infty - v_0)\left(1 - \frac{R_\star}{r}\right)^{\beta}$$

IK Tau β=1.8

W Hya β=5 (Khouri et al.)

W Aql β=2 (Danilovich et al.)

A simple acceleration model assuming dust-driven wind yields β ≈ 0.4-0.7 !!

Any viable mass-loss mechanism must adhere to the behaviour in the acceleration zone !!

The atomic CSE & HI 21cm line

The CSEs ought to be partly atomic, e.g., HI, but this is a difficult observational problem due to the ubiquitous interstellar HI emission.

Conclusions so far from Nancay survey of ≈100 stars of different chemical types, variability types, and mass-loss rates in the HI 21cm line (Gerard, Le Bertre, Libert, et al.):

- High detection rates for low mass-loss rates ($<10^{-7}$ $M_\odot$/yr; irregulars and semi-regulars), but lower for Miras.
- Double-component line profiles: suggesting an expanding, decelerated wind, and a quasi-stationary shell of material that accumulates between the termination shock and the ISM.
- Total HI masses are only of the order few x (10^{-3} - 10^{-2}) $M_\odot$
- HI line centroids are often displaced towards zero velocity (in LSR scale).

Conclusions from VLA imaging of about a dozen sources in HI 21cm line (Matthews et al.):

- Confirm that the HI envelopes are characterised by both their inherent properties and their interaction with the ISM.
- Deceleration of the gas is measured; this gives an age estimate of the mass-losing history of the star.

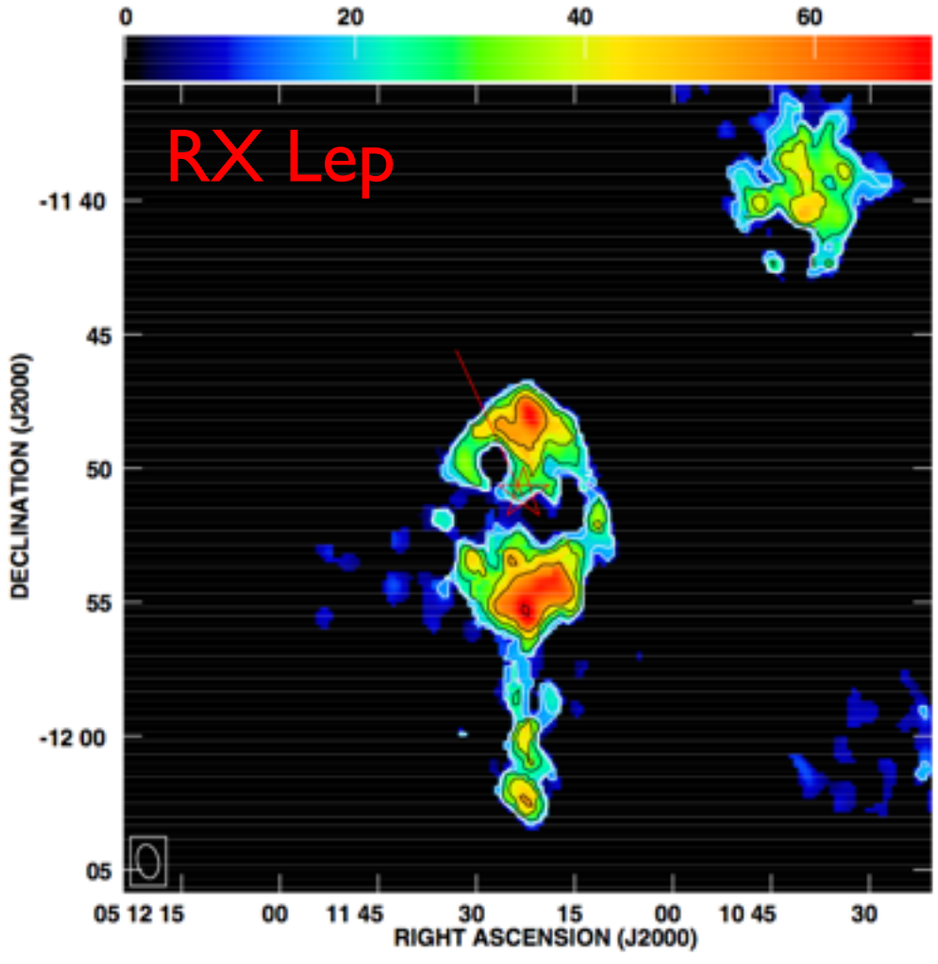

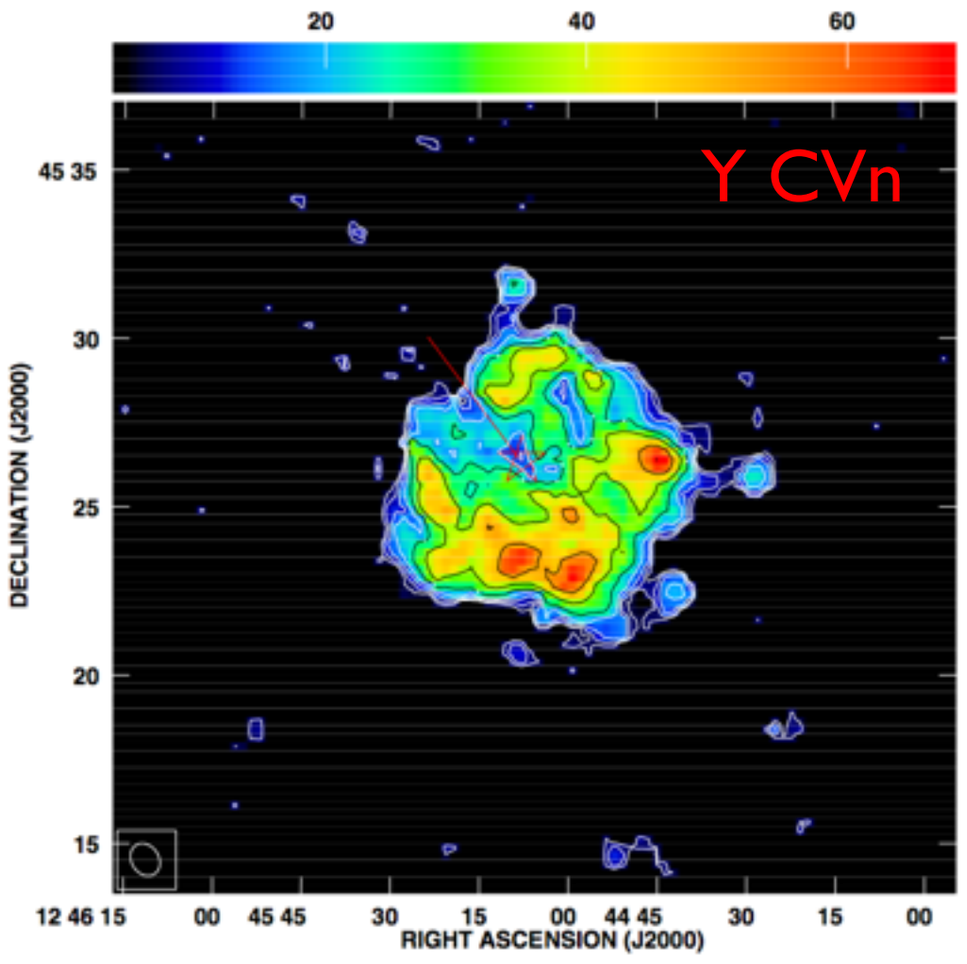

Matthews et al., ApJ 145, 97 (2013)

Chemistry

Table 1: Molecules detected in AGB CSEs

2-atoms:	AlCl	CN	KCl	SiC
	AlF	CP	NaCl	SiN
	AlO	CS	OH	SiO
	C_2	ClH	PN	SiS
	CO	FH	PO	SO
3-atoms:	AlNC	CO_2	HNC	SiC_2
	C_3	FeCN	KCN	SiCN
	C_2H	HCN	MgCN	SiCSi
	C_2N	HCP	MgNC	SiNC
	C_2P	H_2O	NaCN	SO_2
	C_2S	H_2S		
4-atoms:	c-C_3H	C_3S	H_2CS	NH_3
	ℓ-C_3H	C_2H_2	HMgNC	PH_3
	C_3N	HC_2N	MgC_2H (?)	SiC_3
	C_3O	H_2CO	NC_2P (?)	
5-atoms:	C_5	c-C_3H_2	CH_2NH	H_2C_3
	C_4H	CH_2CN	HC_3N	HNC_3
	C_4Si	CH_4	HC_2NC	SiH_4
6-atoms:	C_5H	C_5S	CH_3CN	H_2C_4
	C_5N	C_2H_4	HC_4N	SiH_3CN (?)
$\geq$*7-atoms:*	C_6H	CH_2CHCN	HC_7N	
	C_7H	CH_3CCH	HC_9N	
	C_8H	HC_5N	H_2C_6	
Ions:	C_4H^-	C_6H^-	C_8H^-	HCO^+
	CN^-	C_3N^-	C_5N^-	

The number of detected molecules in AGB-CSEs is impressive: 90 + 3?

To this can be added a few that are unique to the post-AGB objects.

The importance of circumstellar astrochemistry:

- Reasonably well-defined boundary conditions.
- Three different chemistries (C/O<1, ≈1, >1).
- Possibility to do time-resolved chemistry.
- Necessary for estimating elemental abundances of highly obscured objects.
- The possibility to study dust formation in detail.

These studies can be done in different ways!

Unbiased spectral scans

The importance of unbiased spectral scans for understanding circumstellar chemistry must be emphasized !!

The spectral scans at 3, 2, and 1.3 mm of CW Leo (IRC+10216) done at the IRAM 30m telescope have lead to an unprecedented number of new circumstellar molecules detected.

Herschel added to this.

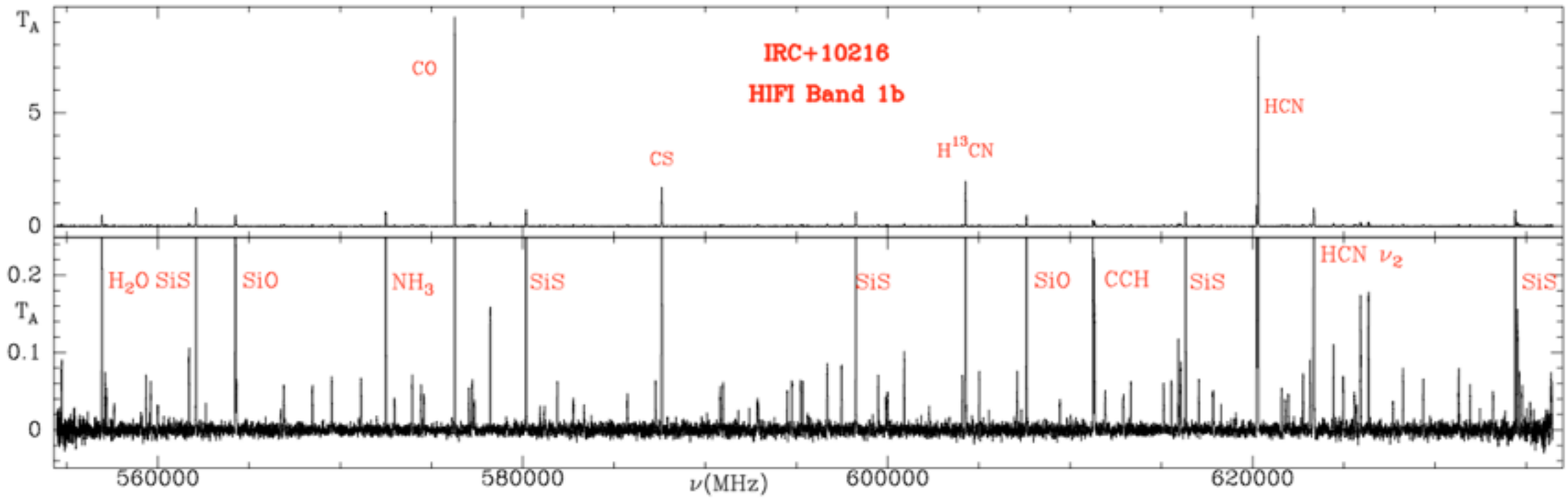

Cernicharo et al., A&A 521, L8 (2010)

Additional C-stars

Zhang et al. (ApJ 691, 1660, 2009):

ARO/SMT spectral scan of RW LMi

131 – 160, 219 – 244, 252 – 268 GHz

74 lines were detected;

5 were unassigned

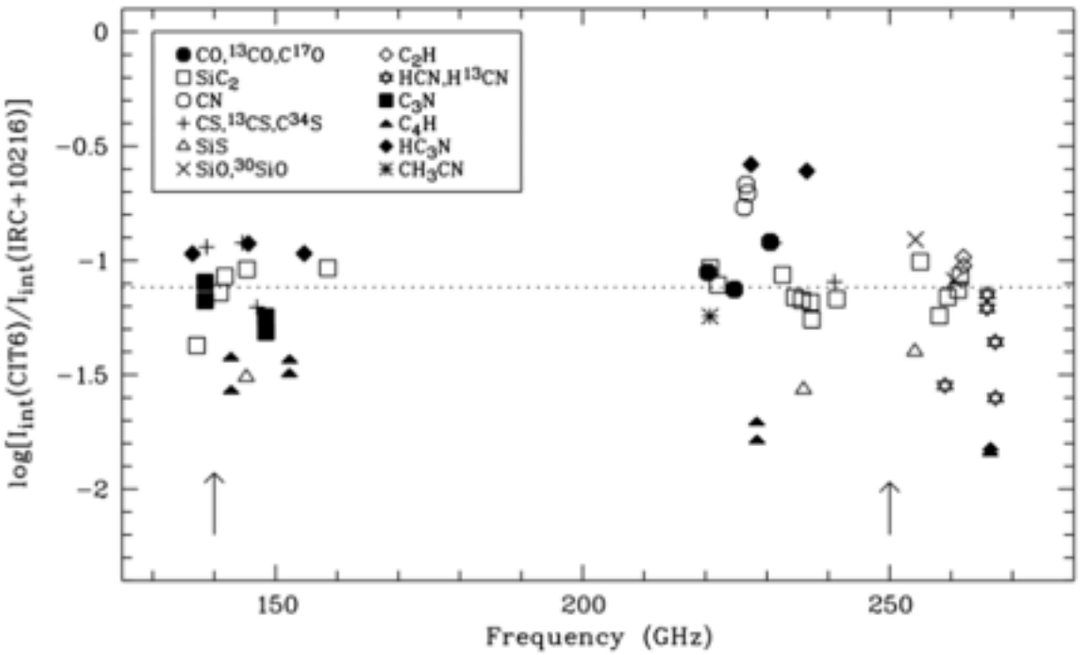

Enhanced emission from CN and HC_3N, depleted emission from HCN, SiS, and C_4H in RW LMi (compared to CW Leo).

Zhang et al. (ApJ 700, 1262, 2009):

ARO/SMT spectral scan of AFGL3068

130 – 162, 220 – 268 GHz

72 lines were detected;

3 were unassigned

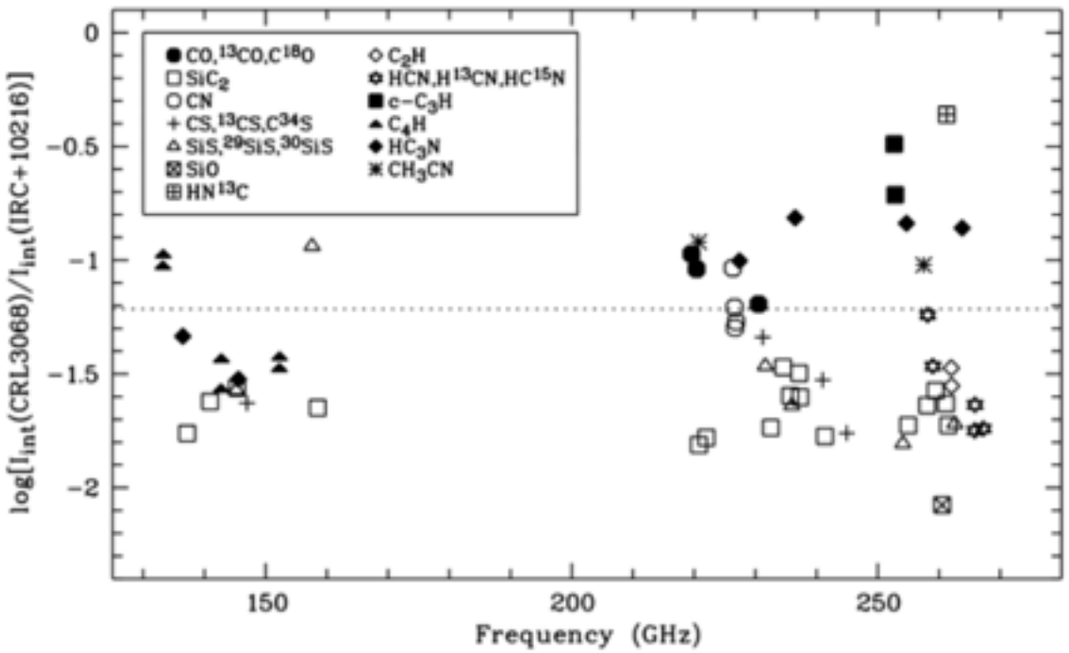

A more extensive synthesis of cyclic and long-chain molecules in AFGL3068 (compared to CW Leo).

Interesting differences between sources are emerging.

See also Chau et al., ApJ 760, 66 (2012)

Also M-stars

Velilla Prieto et al. (A&A 597, A25, 2017) survey of IK Tau:

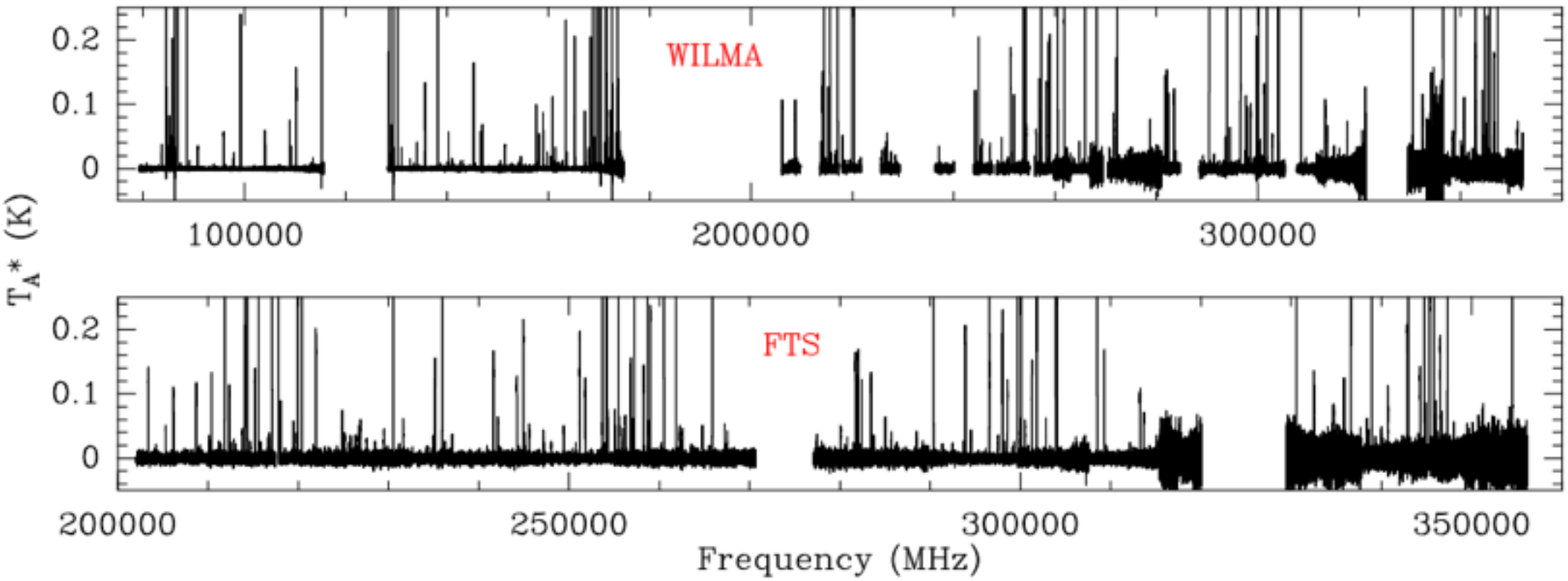

De Beck & Olofsson (in prep) survey of R Dor:

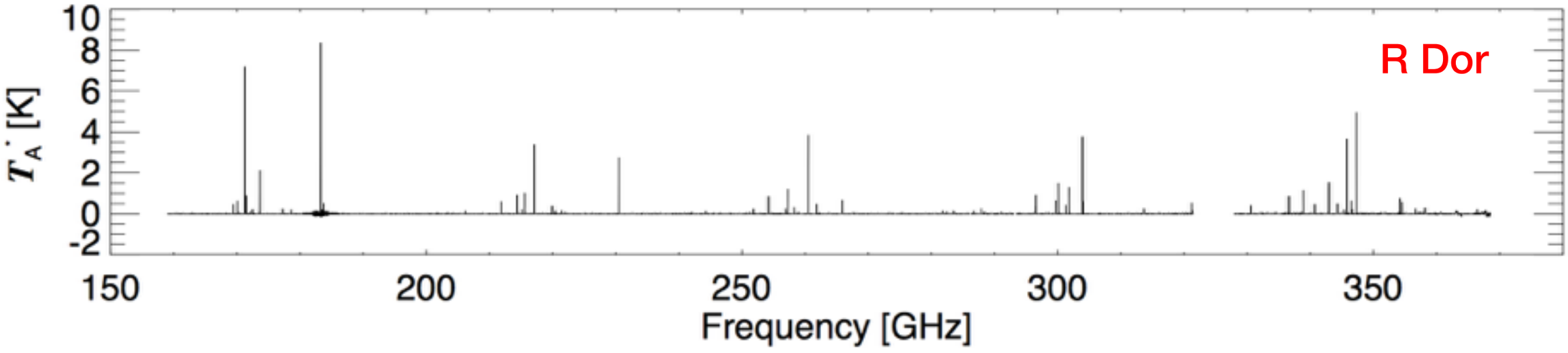

Next step: imaging spectral scans

An example:
ALMA “spectral scan” of CW Leo
Cernicharo et al. (2013)
ApJ 778, L25:

IRAM 30m
single-dish

ALMA
interferometer

Note:
large effect of
resolved out flux !!
&
large number of U-
lines in ALMA data !!

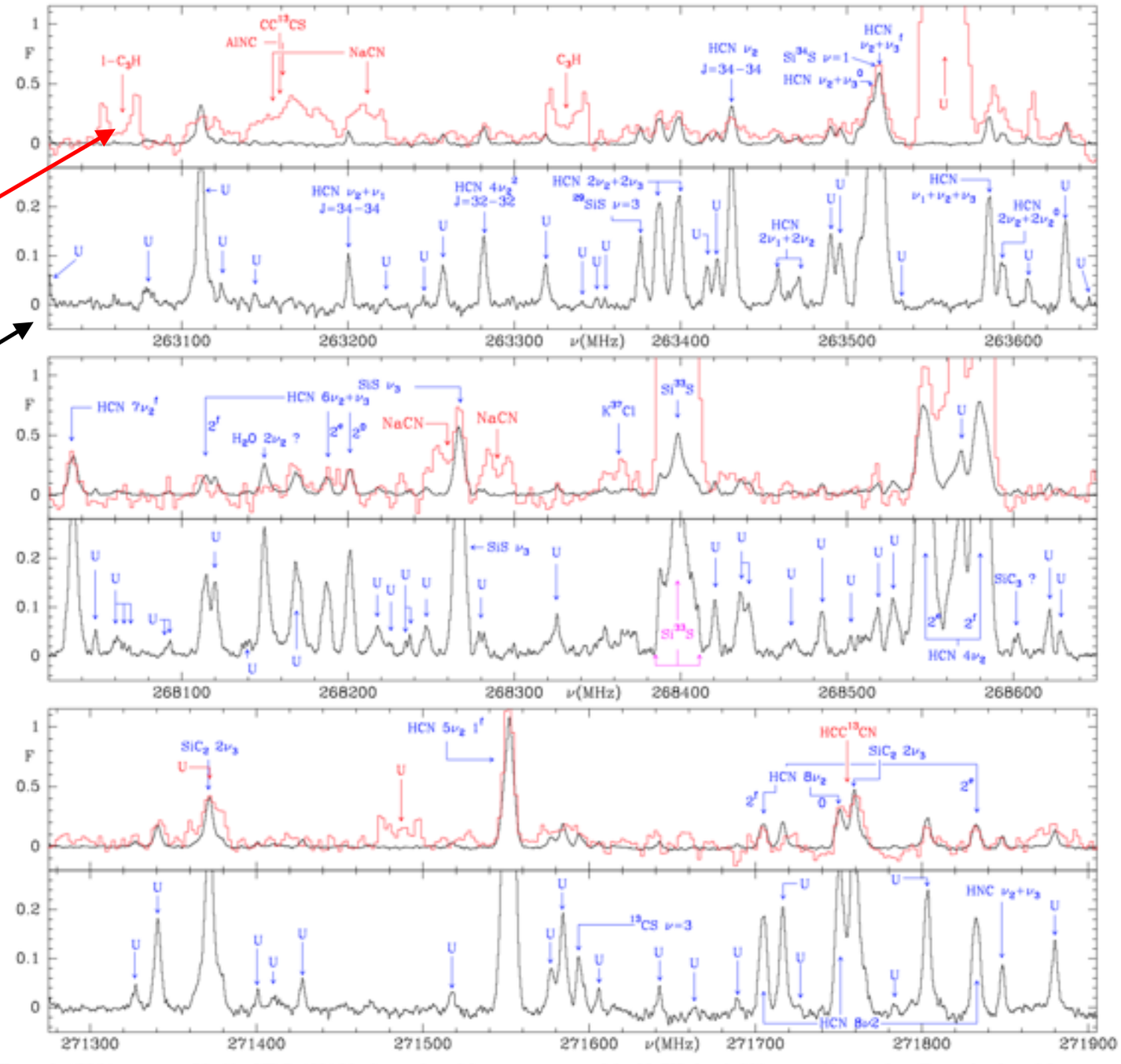

Figure 1. ALMA spectrum (black) of IRC+10216 in three selected frequency ranges of the 20 GHz bandwidth covered by our data. For each selected frequency the ALMA spectrum is compared to the data obtained with the 30-m IRAM telescope (red) at the same frequency (Cernicharo et al. 2011). Intensity scale is in units of Jy Beam^{-1}. Spectral resolution is ~1 MHz for both datasets. The bottom panel of each selected frequency shows a close-up view of the ALMA data. Interestingly, a forest of narrow and unidentified lines are evidenced thanks to the extreme sensitivity, and much higher angular resolution, of ALMA. Note the good calibration agreement for lines spatially unresolved by both instruments. Labels in red correspond to lines detected with the 30-m telescope and filtered by the interferometer.

Some molecules & Imaging & One source

& rad. transfer

C_2H

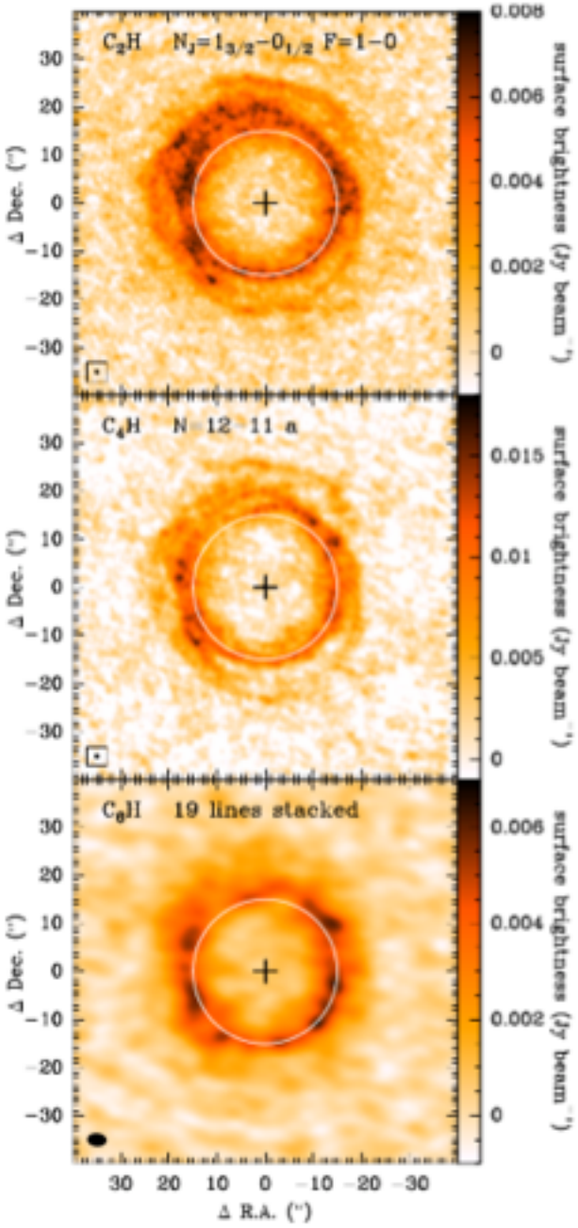

C_4H

C_6H

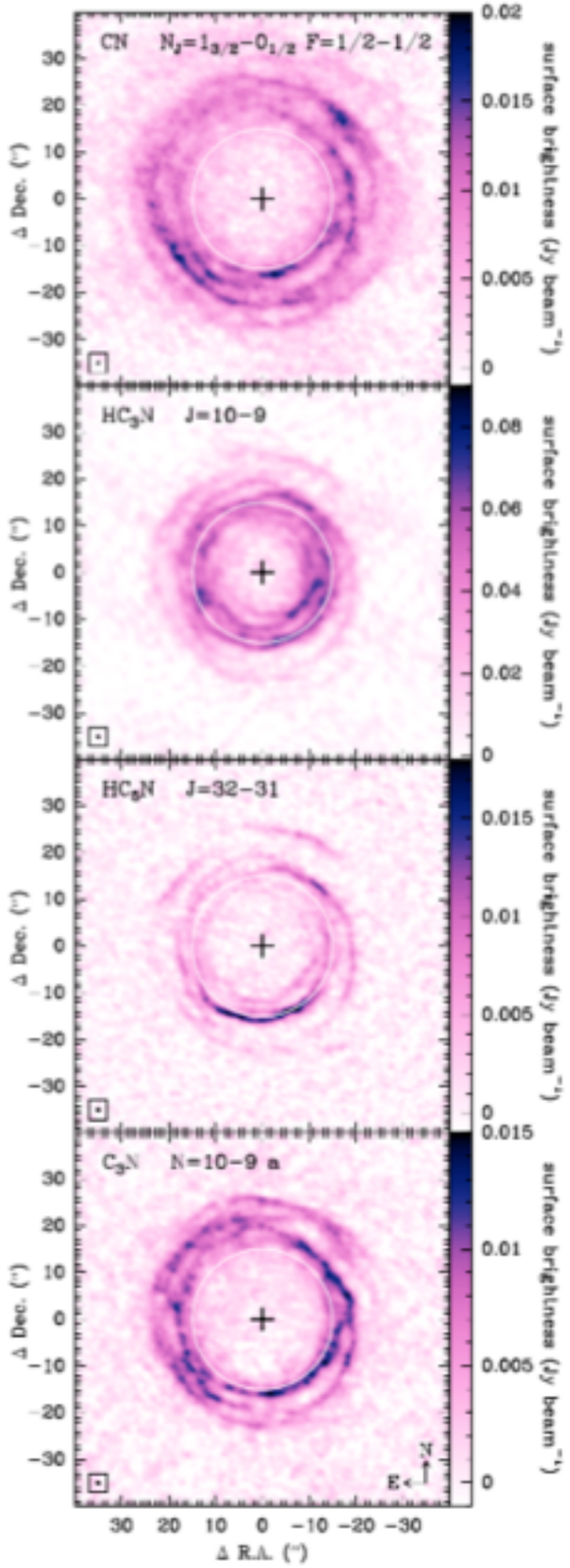

C_2H

HC_3N

HC_5N

C_3N

Imaging of carbon-chain molecules (chemically connected) towards the carbon star CW Leo

Agundez et al., A&A 601, A4 (2017)

Chemical model vs Observations

Process
Bimolecular gas-phase chemical
$C_2H + C_{2n}H_2 \rightarrow C_{2n+2}H_2 + H$
$C_4H + C_{2n}H_2 \rightarrow C_{2n+4}H_2 + H$
$C_2 + C_{2n}H_2 \rightarrow C_{2n+2}H + H$
$CN + C_{2n}H_2 \rightarrow HC_{2n+1}N + H$
$C_3N + C_{2n}H_2 \rightarrow HC_{2n+3}N + H$
Photodissociation processes[b]
$C_2H_2 + h\nu \rightarrow C_2H + H$
$C_4H_2 + h\nu \rightarrow C_4H + H$
$C_6H_2 + h\nu \rightarrow C_6H + H$
$HCN + h\nu \rightarrow CN + H$
$HC_3N + h\nu \rightarrow C_3N + H$
$\rightarrow C_2H + CN$
$HC_5N + h\nu \rightarrow C_5N + H$
$\rightarrow C_4H + CN$

Chemical results and line radiative transfer

Observational results

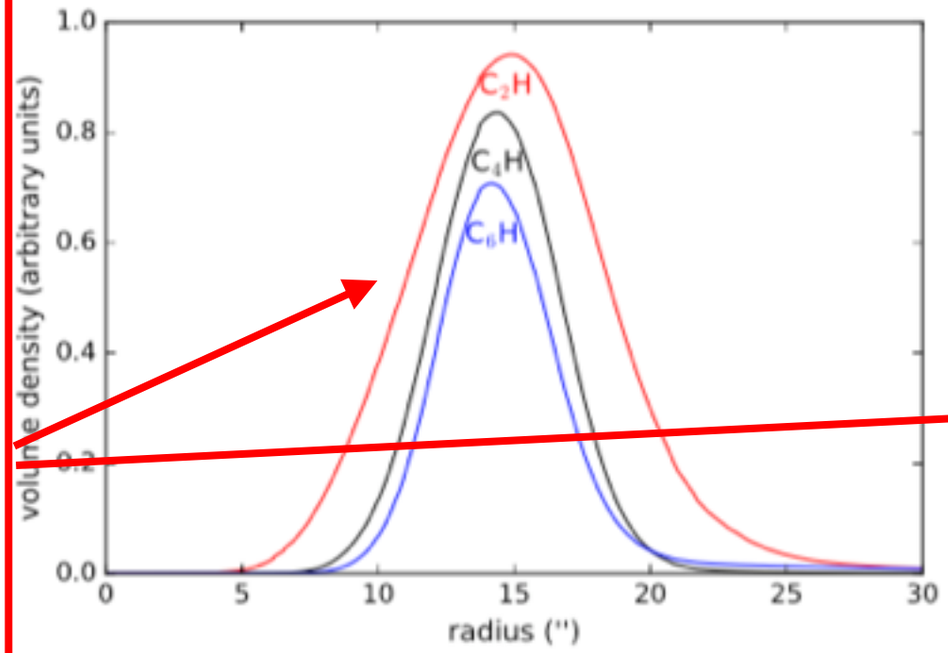

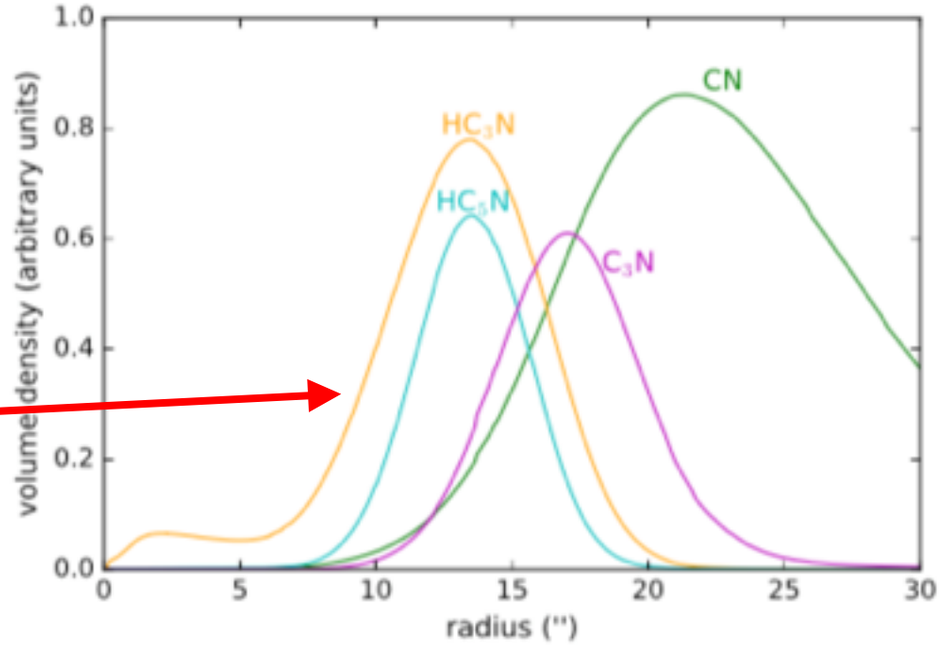

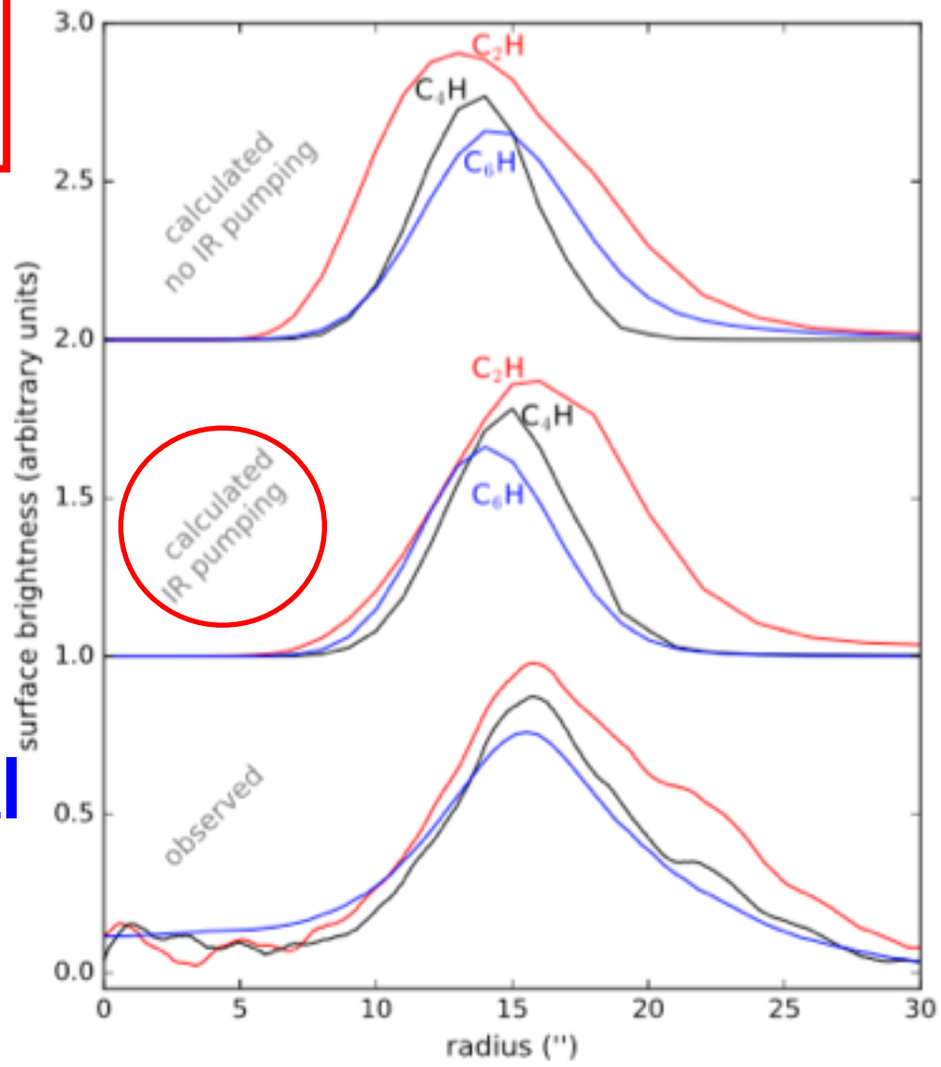

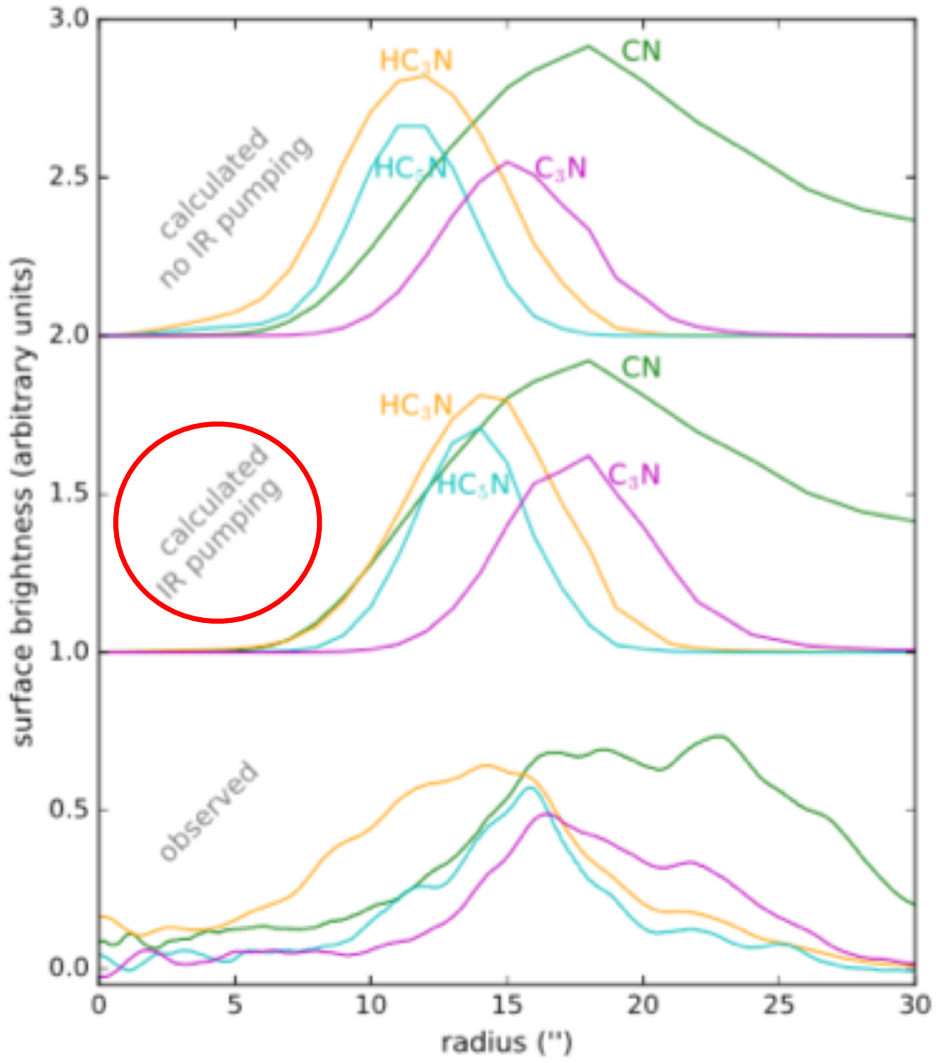

Few molecules & Some lines & Many sources

& rad. transfer

Schöier et al., (A&A 473, 871, 2007; A&A 550, A78, 2013) & Ramstedt et al., (A&A 499, 515, 2009) studied samples of the order 20 M-, 20 S-, and 20 C-stars in HCN, SiO, and SiS.

abundance

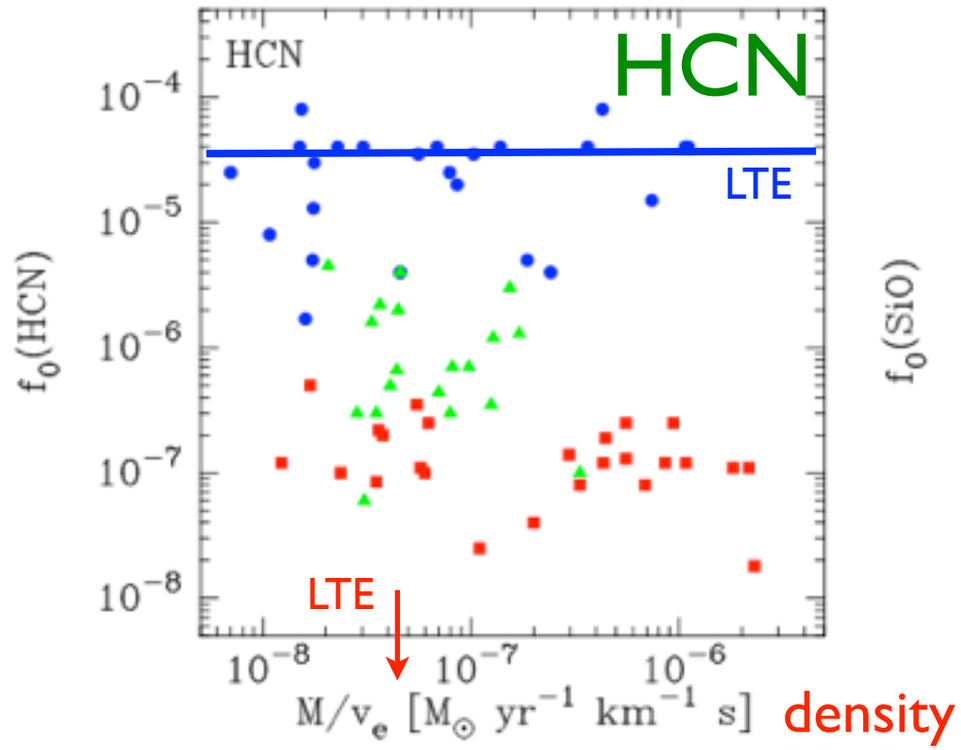

density

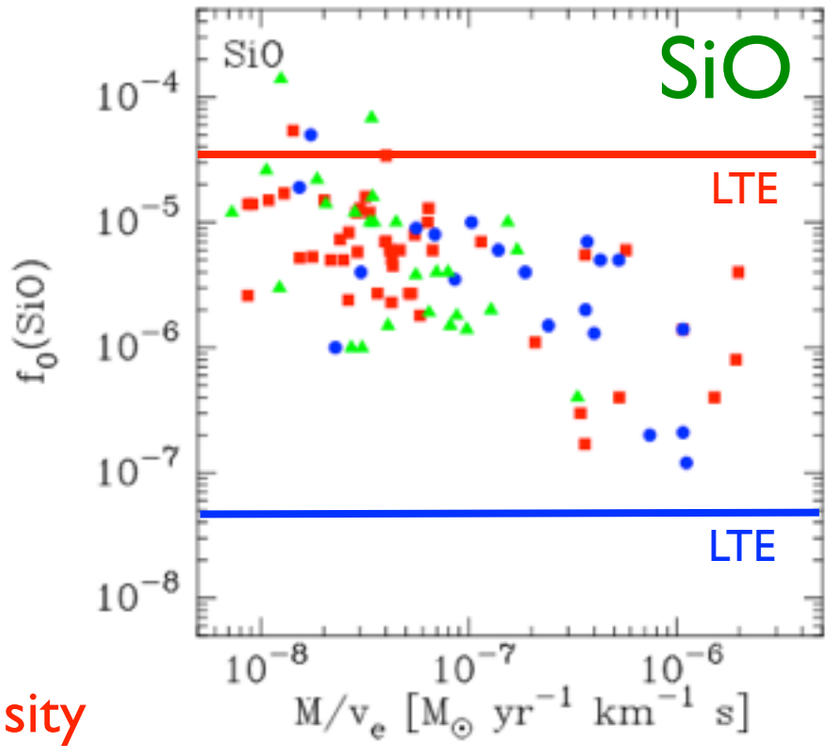

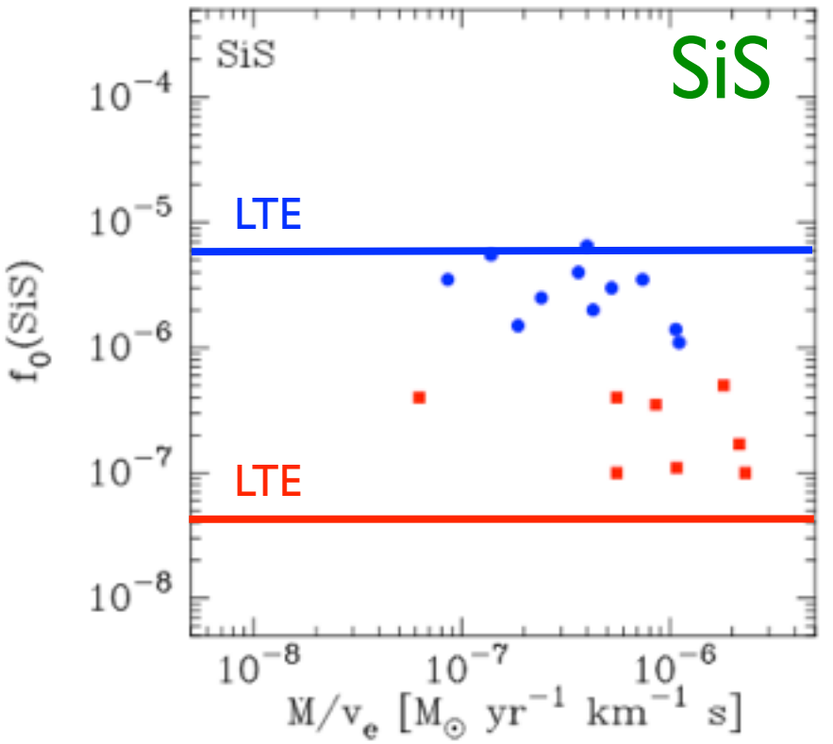

C/O dep.
no dM/dt dep.

no C/O dep.
dM/dt dep.

C/O dep.
no dM/dt dep.

Provide important constraints on chemical models !!

Few molecules & Many lines & One source

& rad. transfer

Observed and model SiO line profiles towards R Dor.

No imaging. E_{up} acts as the radial discriminator.

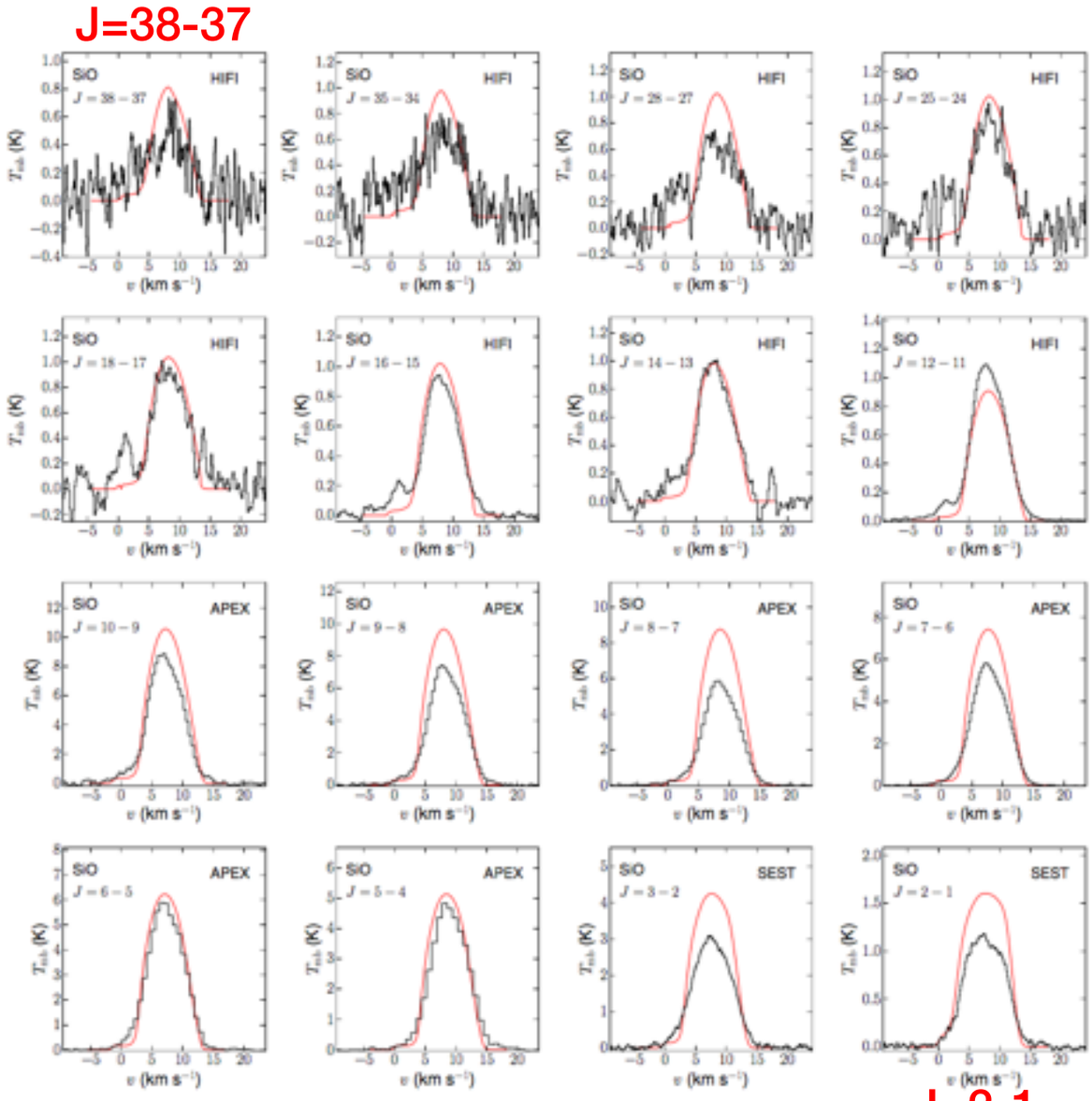

Van de Sande et al., A&A, in press

Comparison of observed and model SiO line intensities.

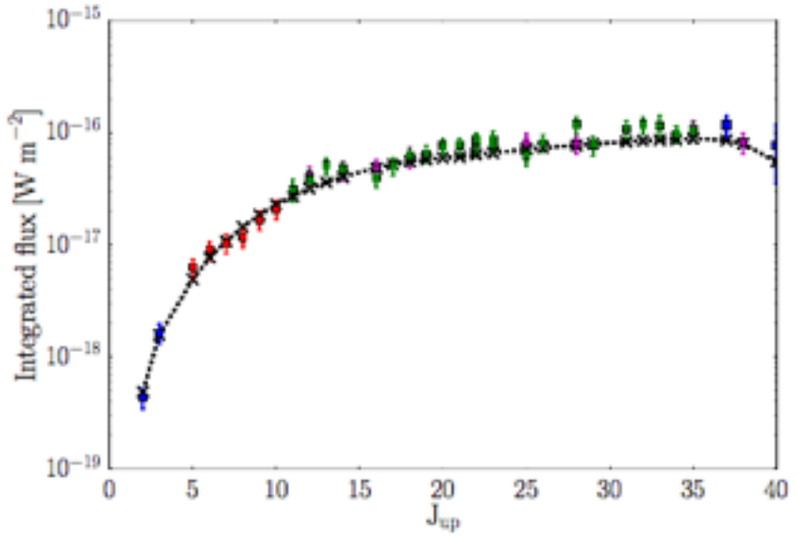

Derived radial SiO abundance distribution.

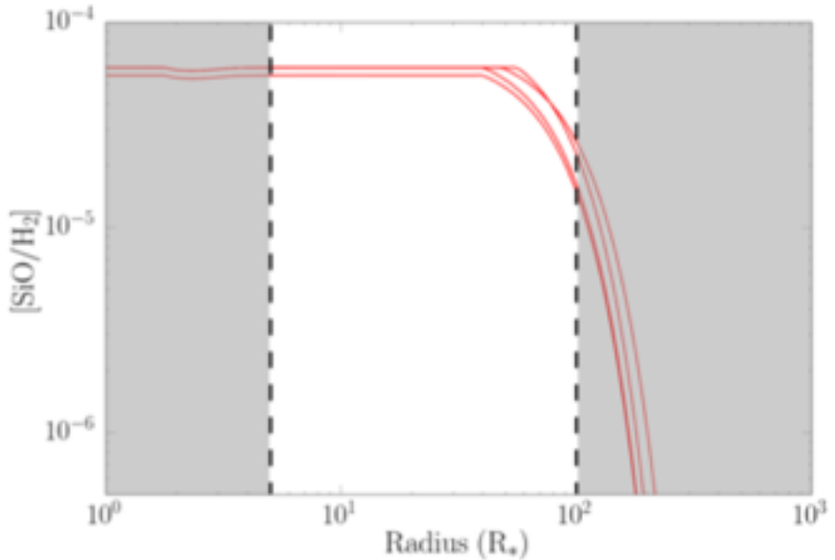

Radial range probed by the observed transitions

Isotopes

Isotope ratios

Isotope ratios are important tracers of stellar nucleosynthesis.

The problem is to convert I(^{n}XA) & I(^{m}YA) into [^{n}X] & [^{m}Y], i.e., molecular isotopologue ratios into elemental isotope ratios

A number of things need to be considered:

- Optical depths
- Isotope-different excitation (in some cases masering)
- Isotope-selective photodissociation
- Chemical fractionation

Circumstellar ^{12}C and ^{13}C

Ramstedt & Olofsson (A&A 566, A145, 2014) have presented an extensive study of circumstellar ^{12}CO and ^{13}CO: 19 M-, 17 S-, and 19 C-stars

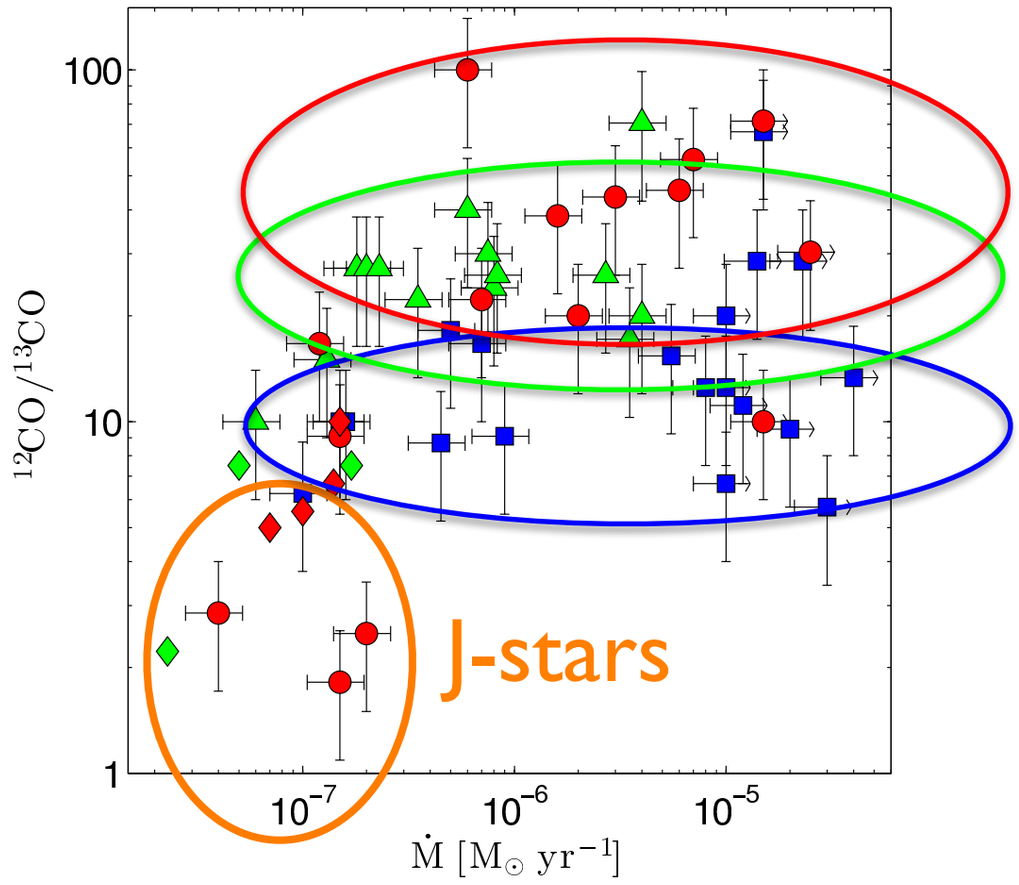

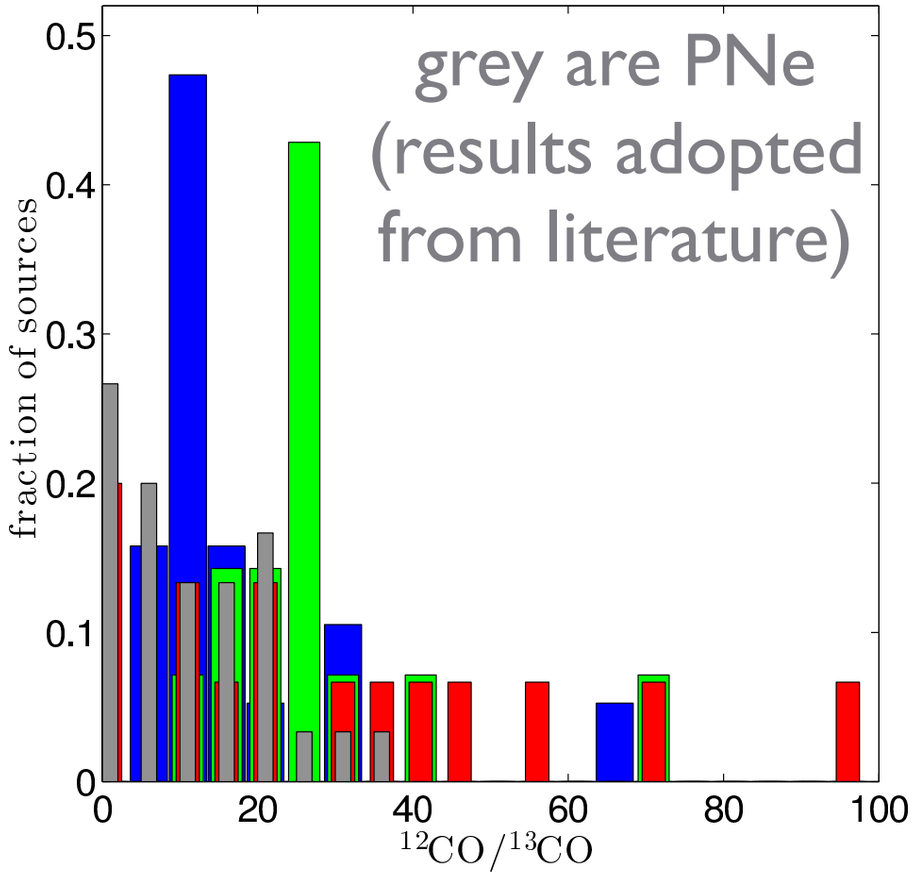

- The three chemical types have (on average) different $^{12}CO/^{13}CO$ as expected when evolving from M to C via S.
- No dependence on mass-loss rate.
- The J-stars are very different from the rest.
- PNe come from the low $^{12}CO/^{13}CO$ objects.

Circumstellar ^{16}O, ^{17}O, and ^{18}O

The $^{17}O/^{18}O$ ratio is an initial mass estimator for M < 4 $M_\odot$!!

C-star limit

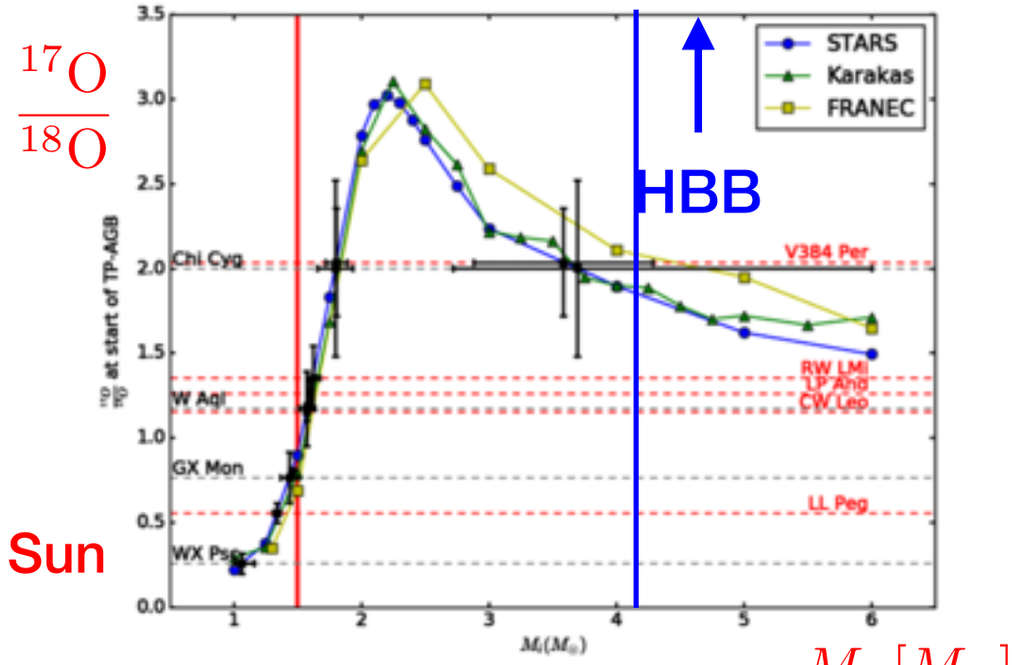

deNutte et al. (A&A 600, A71, 2017)

9 AGB stars with both C^{17}O and C^{18}O

+ some objects with only C^{18}O

Studies of the rarer isotopes are reaching their limits on single telescopes !!

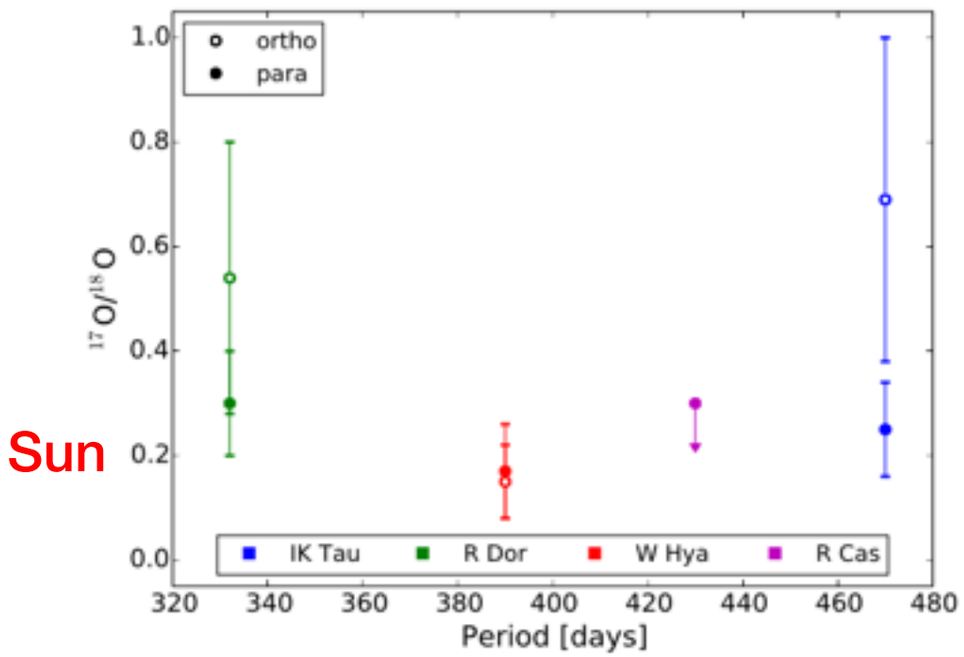

Danilovich et al. (A&A 602, A14, 2017)

4 AGB stars with both $H_2{}^{17}O$ and $H_2{}^{18}O$

The $^{17}O/^{18}O$ ratio is also a discriminator between low- and "high"-mass stars due to the hot-bottom-burning process (destroys effectively ^{18}O) !!

Miras

OH/IR

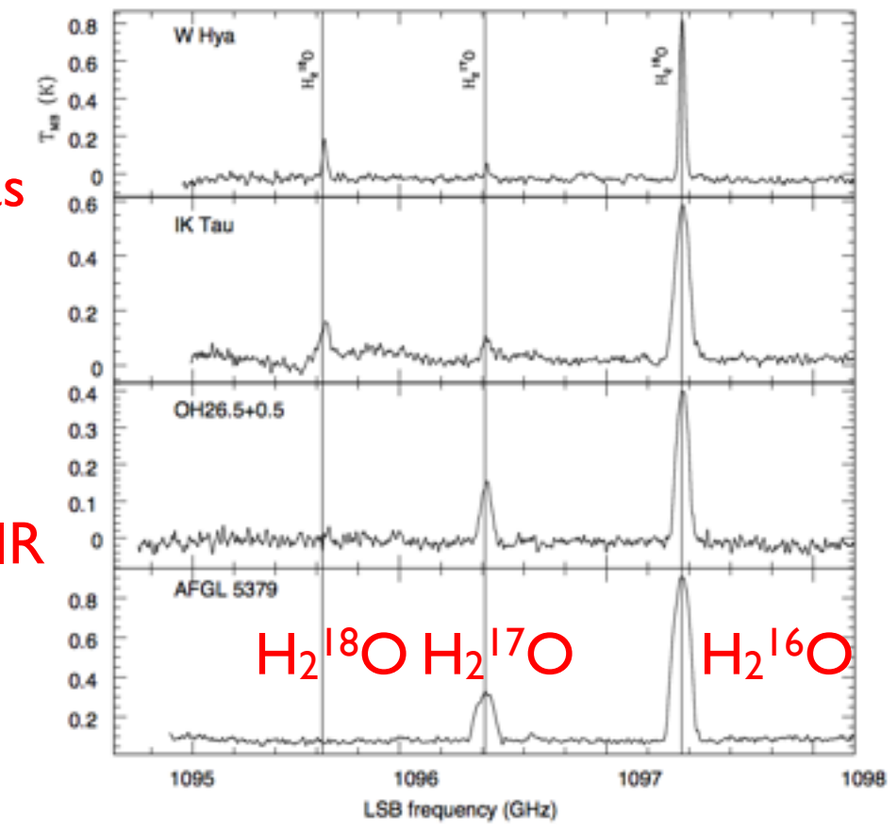

9 OH/IR stars, only $H_2{}^{17}O$ detected

In general, $I(H_2{}^{18}O)/I(H_2{}^{17}O) < 0.1$

These are massive stars, $>5M_\odot$

Justtanont et al., A&A 578, A115 (2015)

Multi-isotope studies of individual sources

CW Leo

Table 1: Isotope ratios in the CSE of IRC+10216

Isotope ratio	Ratio	IRC/Solar	Species used
$^{12}C/^{13}C$	45	0.5	CS
$^{12}C/^{14}C$	> 63000		CO
$^{14}N/^{15}N$	5300	20	HCN
$^{16}O/^{17}O$	840	0.3	CO
$^{16}O/^{18}O$	1300	3	CO
$^{28}Si/^{29}Si$	18	0.9	SiO, SiS
$^{28}Si/^{30}Si$	27	0.9	SiO, SiS
$^{32}S/^{33}S$	110	1	SiS
$^{32}S/^{34}S$	22	1	SiS
$^{32}S/^{36}S$	2700	0.4	CS
$^{35}Cl/^{37}Cl$	3.0	1	AlCl, HCl, NaCl, KCl
$^{24}Mg/^{25}Mg$	8	1	MgNC
$^{24}Mg/^{26}Mg$	7	1	MgNC

CW Leo, RW LMi, AFGL3068

Table 3
Isotopic Abundance Ratios

Isotopic Ratio	CRL 3068		CIT 6[a]	IRC+10216[b]	Solar[c]
	Species	Value			
$^{12}C/^{13}C$	$^{12}C^{34}S/^{13}C^{32}S$	29.7[d]	45.4	45	89
	$^{12}CO/^{13}CO$	5.6[e]	...	...	...
	$^{12}CS/^{13}CS$	9.8[e]	...	...	...
	$H^{12}CN/H^{13}CN$	1.2[e]	...	...	...
$^{14}N/^{15}N$	$H^{13}C^{14}N/H^{12}C^{15}N$	1099[f]	...	...	272
	$HC^{14}N/HC^{15}N$	45[e]	...	...	...
$^{16}O/^{17}O$	$^{13}C^{16}O/^{12}C^{17}O$	668:[f]	890	967	2680
	$C^{16}O/C^{17}O$	125:[e]	...	...	...
$^{16}O/^{18}O$	$^{13}C^{16}O/^{12}C^{18}O$	472[f]	...	1172	499
	$C^{16}O/C^{18}O$	88[e]	...	...	...
$^{17}O/^{18}O$	$C^{17}O/C^{18}O$	0.7:	...	1.14	0.2
$^{32}S/^{34}S$	$C^{32}S/C^{34}S$	7.4[e]	6.7[e]	18.9	22.5
$^{33}S/^{34}S$	$C^{33}S/C^{34}S$	0.3:	0.2:	0.19	0.18
$^{29}Si/^{30}Si$	$^{29}SiS/^{30}SiS$	2.5	1.0	1.46	1.52
$^{28}Si/^{30}Si$	$^{28}SiS/^{30}SiS$	28.8	8.8[e]	24.7	29.9
$^{28}Si/^{29}Si$	$^{28}SiS/^{29}SiS$	11.5	8.9[e]	17.2	19.6

Notes.
[a] From Zhang et al. (2009).
[b] From He et al. (2008) except the $^{12}C/^{13}C$ ratio which was taken from Cernicharo et al. (2000).
[c] From Lodders (2003).
[d] Assume that the $^{34}S/^{32}S$ ratio is solar.
[e] Should be treated as lower limits due to opacity effect.
[f] Adopted: $^{12}C/^{13}C = 29.7$.

Zhang et al. , ApJ 700, 1262 (2009)

Disks

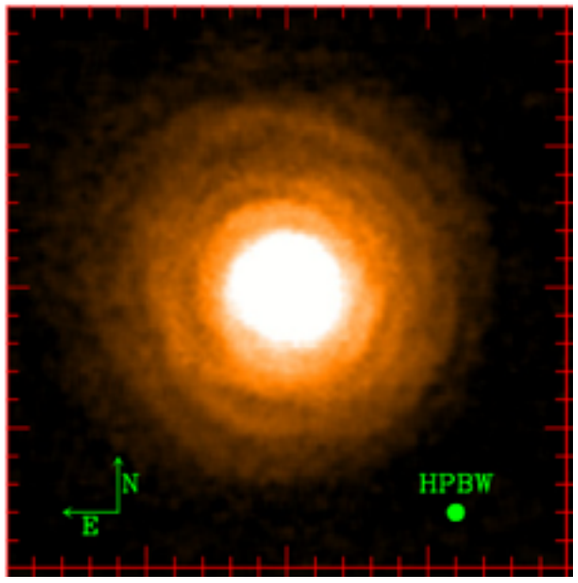

Presence of disks already during the AGB is of great interest for the possible future evolution to a planetary nebula.

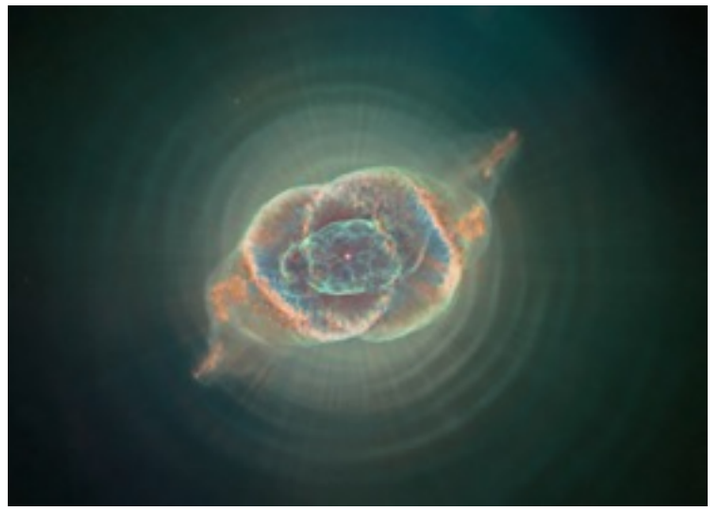

L_2 Pup is the only AGB star with a detected disk.

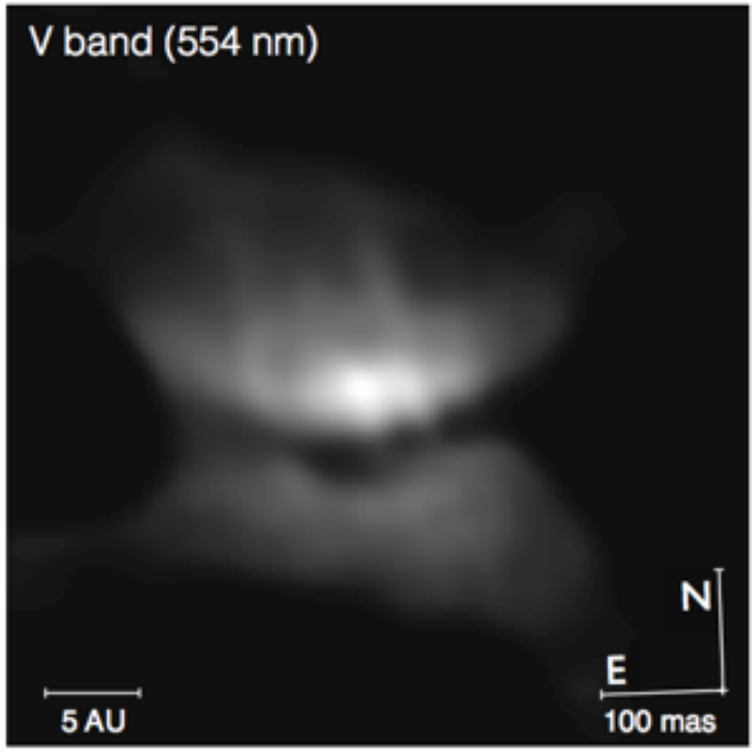

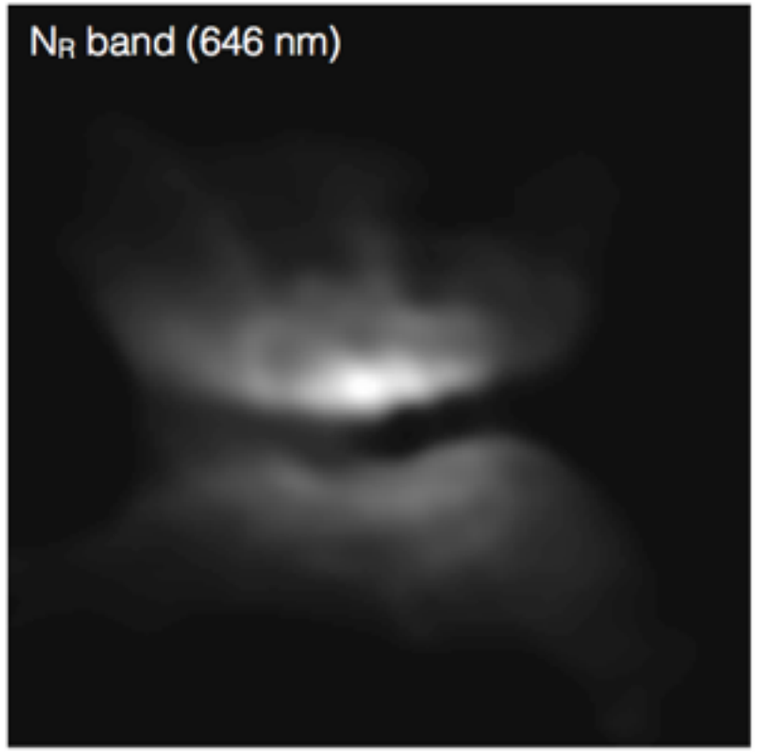

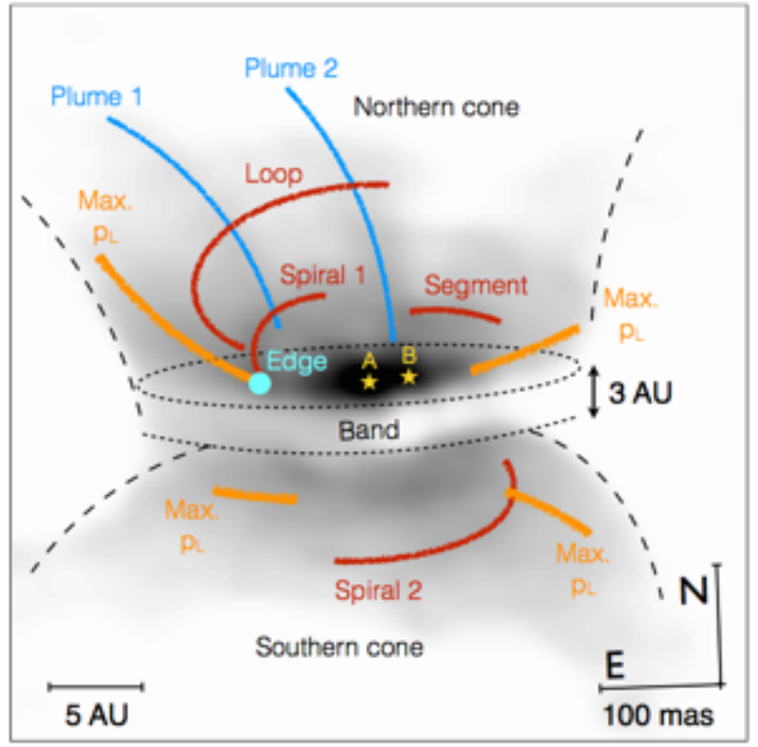

Lykou et al., A&A 576, A46 (2015); Kervella et al., A&A 578, A77 (2015)

ALMA data reveal that the disk is (partly) in Keplerian rotation (18x15 mas resolution).

The current mass of L2 Pup is estimated to be 0.66 $M_\odot$.
Its initial mass was ≈ 1 $M_\odot$. A very solar-like star.

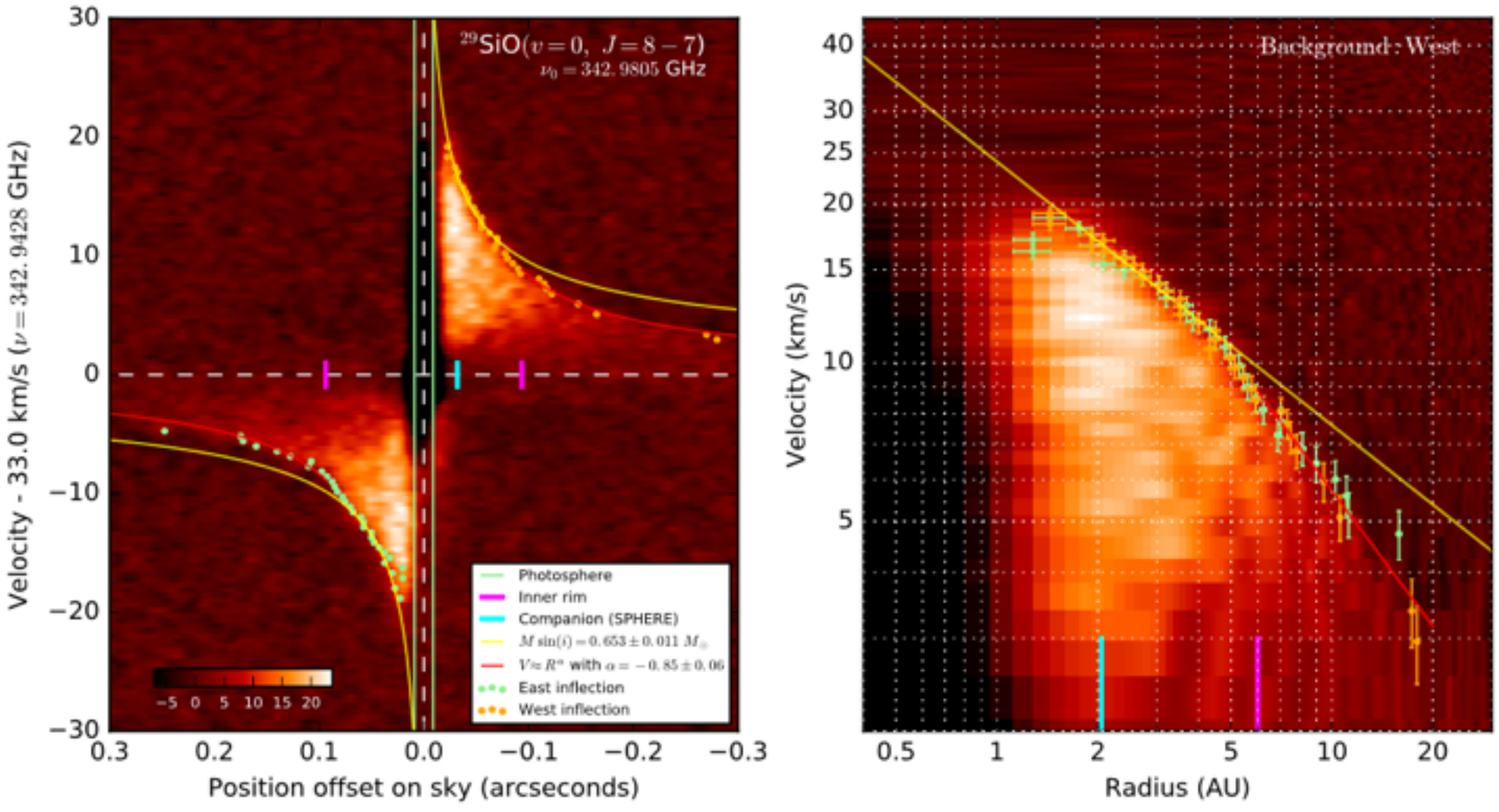

Kervella et al., A&A 596, A92 (2016); also Homan et al., A&A 601, A5 (2017)

ALMA detects also a companion

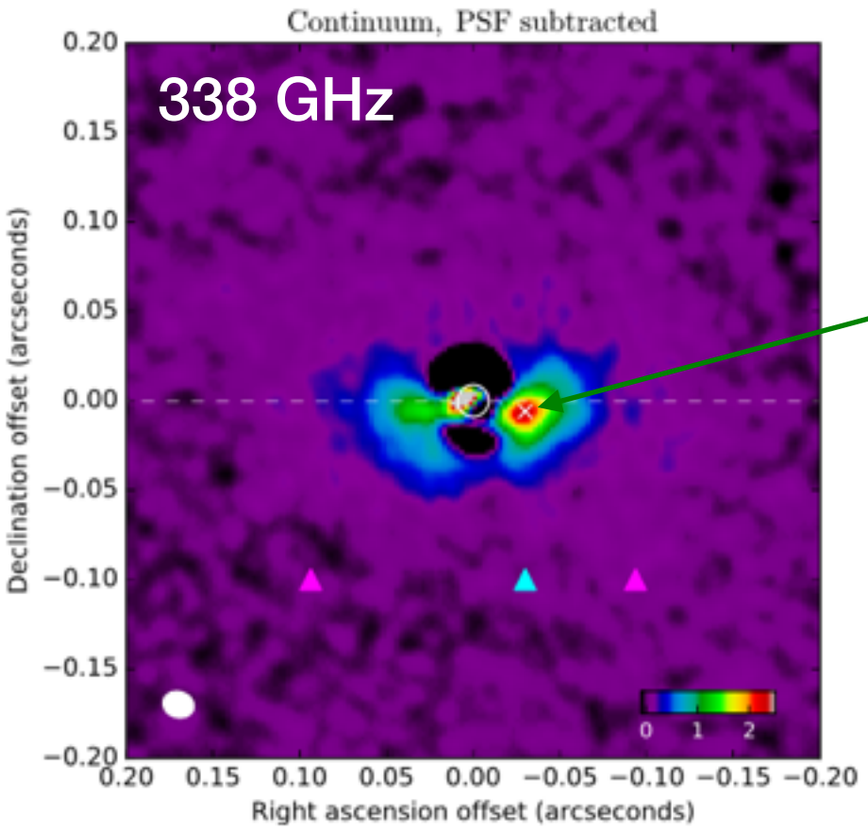

The companion is detected in continuum and in ^{12}CO(3–2) line.

Its mass is estimated to be 12 +/- 16 M_J.

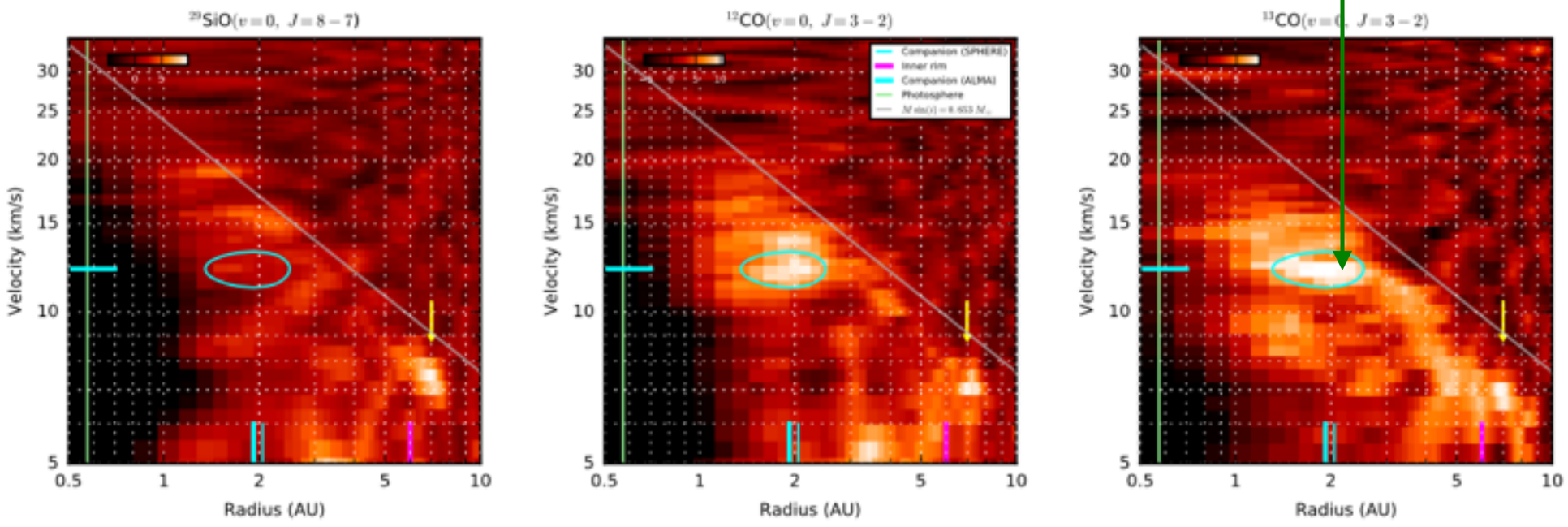

Fig. 8. Position-velocity diagrams of the ^{29}SiO($v = 0, J = 8–7$), ^{12}CO($v = 0, J = 3–2$) and ^{13}CO($v = 0, J = 3–2$) lines for the west part of the gaseous disk from which the east part of the PVD has been subtracted. The cyan ellipse is centered on the position of B, with a radial extension corresponding to the beam size and a velocity range of 12.2 ± 1.0 km s^{-1}. The yellow arrow indicates the position of the notch at 7 AU in the gaseous disk. The color scale is in mJy beam^{-1}.

Kervella et al., A&A 596, A92 (2016)

Magnetic fields

Polarisation

Hopefully radio interferometers can contribute significantly in this field through polarisation measurements (maser as well as non-maser lines).

- The Zeeman effect (e.g. SiO, H2O, OH, CN)
- Goldreich-Kylafis effect (e.g. CO)

Important characteristics:

- Magnetic field strength vs r
- Magnetic field shape
- Origin of magnetic field
- Importance of binarity

Critical to understand the possible importance of magnetic fields for the mass-loss characteristics and the post-AGB evolution.

Only measured value
for an AGB star
(χ Cyg, an S-star)

M-stars

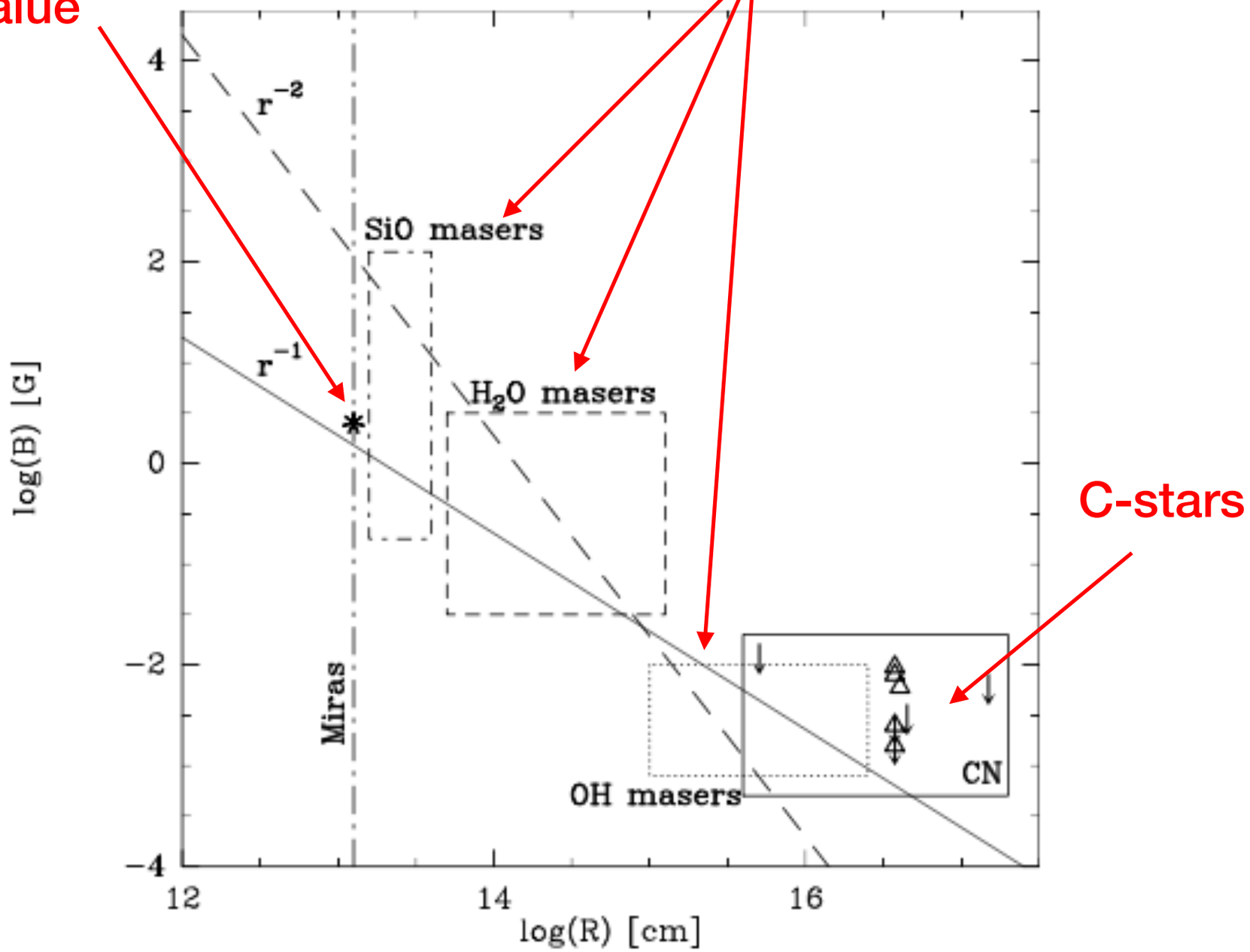

C-stars

Vlemmings, IAU Symp. 287, 31 (2012); Duthu et al., A&A 604, A12 (2017)

Thank you!